Published for SISSA by Springer

Received: *March 10, 2023*
Accepted: *June 19, 2023*
Published: *July 13, 2023*

Search for third-generation vector-like leptons in pp collisions at $\sqrt{s} = 13$ TeV with the ATLAS detector

The ATLAS collaboration

E-mail: atlas.publications@cern.ch

Abstract: A search for vector-like leptons in multilepton (two, three, or four-or-more electrons plus muons) final states with zero or more hadronic τ-lepton decays is presented. The search is performed using a dataset corresponding to an integrated luminosity of 139 fb^{-1} of proton-proton collisions at a centre-of-mass energy of 13 TeV recorded by the ATLAS detector at the LHC. To maximize the separation of signal and background, a machine-learning classifier is used. No excess of events is observed beyond the Standard Model expectation. Using a doublet vector-like lepton model, vector-like leptons coupling to third-generation Standard Model leptons are excluded in the mass range from 130 GeV to 900 GeV at the 95% confidence level, while the highest excluded mass is expected to be 970 GeV.

Keywords: Beyond Standard Model, Hadron-Hadron Scattering, Tau Physics

ArXiv ePrint: 2303.05441

https://doi.org/10.1007/JHEP07(2023)118

JHEP07(2023)118

Contents

1 Introduction

The predictions of the Standard Model (SM) of particle physics are in excellent agreement with measurements of proton-proton (pp) collisions at the Large Hadron Collider (LHC) [1]. Nonetheless, some aspects of our universe cannot be explained within the framework of the SM, such as the excess of matter over antimatter, the origin of the neutrino masses, the nature of dark matter and dark energy, and the hierarchy and fine-tuning problems [2, 3]. Many possible ways to find solutions have been proposed, including models based on supersymmetry, which help to explain why the Higgs boson's mass is very far from the Planck scale. However, the measured Higgs boson branching fractions are in good agreement with the SM predictions, so it is not easy to accommodate new particles whose masses are generated via the Higgs mechanism [4–6]. One class of particles that are motivated by a variety of phenomenological models based on string theory or large extra dimensions are vector-like fermions that transform as non-chiral representations of the unbroken SM gauge group [7]. They therefore have Dirac masses and decouple from the electroweak scale in the large-mass limit.

A large number of searches for vector-like quarks have been performed at the Tevatron [8, 9] and the LHC [10–27]. In addition, the CMS Collaboration has performed a search for vector-like leptons (VLL) in the τ plus three b-jet final state [28]. The search was performed in the context of the "4321 model" [29–31] over a mass range of 500 to 1050 GeV. Following the suggestion in refs. [32, 33], a search for VLL in a doublet model has been performed by ATLAS and is presented in this article. A similar search was performed by the CMS

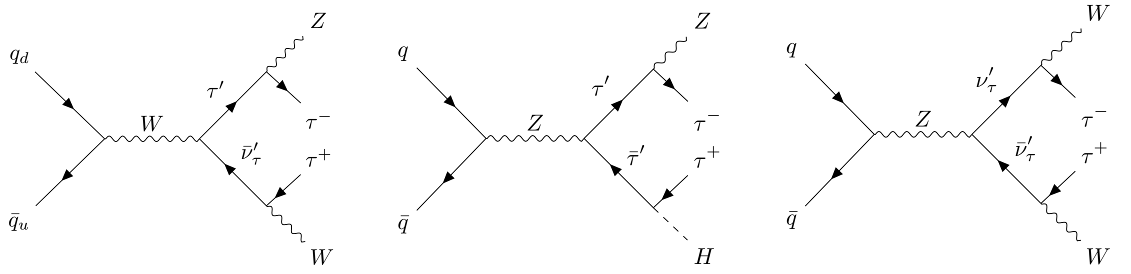

(a) (b) (c)

Figure 1. Examples of LO Feynman diagrams for VLL production and decay: (a) $\tau'\bar{\nu}'_\tau$ production followed by τ' decay into $Z\tau$ and ν'_τ decay into τ^+W^-, where q_u (q_d) represents a weak isospin $+1/2$ ($-1/2$) quark, (b) production of $\tau'\bar{\tau}'$ followed by the decay into $Z\tau^-$ and τ^+H, and (c) $\nu'_\tau\bar{\nu}'_\tau$ production followed by ν'_τ decay into $W\tau$.

Collaboration using 138 fb^{-1} of pp collisions at $\sqrt{s} = 13$ TeV and excludes vector-like τ-lepton masses below 1045 GeV at the 95% confidence level (CL) [34]. The VLL doublet $L' = (\nu_\tau{}', \tau')$ comprises two fermions of approximately equal mass that couple only to the third-generation leptons. The VLL production cross section is dominated by $pp \to \nu_\tau{}'\tau'$, which is approximately 3.7 times greater than either the $pp \to \tau'^+\tau'^-$ or $pp \to \nu_\tau{}'\overline{\nu}_\tau{}'$ modes, which have approximately equal cross sections. The $\nu_\tau{}'$ decays exclusively into $W^+\tau^-$, while the τ' decays are $\tau'^- \to Z\tau^-$ and $\tau'^- \to H\tau^-$, where the branching fraction of the former is larger, but they asymptotically approach each other with increasing τ' mass ($M_{\tau'}$) due to the Goldstone equivalence principle [35]. Examples of leading-order (LO) Feynman diagrams for VLL production and decay are displayed in figure 1. Given the possible decays, the search is performed by selecting events containing at least two charged light leptons, $e^\pm$ or $\mu^\pm$, zero or more τ-leptons decaying hadronically, and a momentum imbalance transverse to the beam. To achieve better background rejection than is possible with an event selection based on kinematic and topological variables, a boosted decision tree (BDT) algorithm is utilized as an event classifier [36, 37].

This article is organized as follows. A brief description of the ATLAS detector is given in section 2. Section 3 presents the data and simulation samples used in this search. The reconstruction of objects used in the search for a VLL signal is delineated in section 4. Section 5 describes techniques used to perform the event selection, while section 6 outlines the method used to estimate the backgrounds. A discussion of the systematic uncertainties is given in section 7. The statistical method used to arrive at the 95% CL upper limit on the VLL production cross section, and hence the mass exclusion region, is described in section 8. Finally, the analysis and results are summarized in section 9.

JHEP07(2023)118

2 ATLAS detector

The ATLAS detector [38] at the LHC covers nearly the entire solid angle around the collision point.[1] It consists of an inner tracking detector surrounded by a thin superconducting solenoid, electromagnetic and hadron calorimeters, and a muon spectrometer incorporating three large superconducting air-core toroidal magnets.

The inner-detector system (ID) is immersed in a 2 T axial magnetic field and provides charged-particle tracking in the range $|\eta| < 2.5$. The high-granularity silicon pixel detector covers the vertex region and provides up to four measurements per track, the first hit normally being in the insertable B-layer (IBL) installed before Run 2 [39, 40]. It is followed by the silicon microstrip tracker (SCT), which usually provides eight measurements per track. These silicon detectors are complemented by the transition radiation tracker (TRT), which enables radially extended track reconstruction up to $|\eta| = 2.0$. The TRT also provides electron identification information based on the fraction of hits (typically 30 in total) above a higher energy-deposit threshold corresponding to transition radiation.

The calorimeter system covers the pseudorapidity range $|\eta| < 4.9$. Within the region $|\eta| < 3.2$, electromagnetic calorimetry is provided by barrel and endcap high-granularity lead/liquid-argon (LAr) calorimeters, with an additional thin LAr presampler covering $|\eta| < 1.8$ to correct for energy loss in material upstream of the calorimeters. Hadron calorimetry is provided by the steel/scintillator-tile calorimeter, segmented into three barrel structures within $|\eta| < 1.7$, and two copper/LAr hadron endcap calorimeters. The solid angle coverage is completed with forward copper/LAr and tungsten/LAr calorimeter modules optimized for electromagnetic and hadronic energy measurements, respectively.

The muon spectrometer (MS) comprises separate trigger and high-precision tracking chambers measuring the deflection of muons in a magnetic field generated by the superconducting air-core toroidal magnets. The field integral of the toroids ranges between 2.0 and 6.0 T m across most of the detector. A set of precision chambers covers the region $|\eta| < 2.7$ with three layers of monitored drift tubes, complemented by cathode-strip chambers in the forward region, where the particle flux is highest. The muon trigger system covers the range $|\eta| < 2.4$ with resistive-plate chambers in the barrel, and thin-gap chambers in the endcap regions.

Interesting events are selected by the first-level trigger system implemented in custom hardware, followed by selections made by algorithms implemented in software in the high-level trigger [41]. The first-level trigger accepts events from the 40 MHz bunch crossings at a rate below 100 kHz, which the high-level trigger further reduces in order to record events to disk at about 1 kHz.

[1] ATLAS uses a right-handed coordinate system with its origin at the nominal interaction point (IP) in the centre of the detector and the z-axis along the beam pipe. The x-axis points from the IP to the center of the LHC ring, and the y-axis points upwards. Cylindrical coordinates (r, ϕ) are used in the transverse plane, ϕ being the azimuthal angle around the z-axis. The pseudorapidity is defined in terms of the polar angle θ as $\eta = -\ln\tan(\theta/2)$. Angular distance is measured in units of $\Delta R \equiv \sqrt{(\Delta\eta)^2 + (\Delta\phi)^2}$.

JHEP07(2023)118

An extensive software suite [42] is used in data simulation, in the reconstruction and analysis of real and simulated data, in detector operations, and in the trigger and data acquisition systems of the experiment.

3 Data and simulation samples

The data sample used in this article corresponds to an integrated luminosity of 139 fb^{-1} of pp collisions at a centre-of-mass energy ($\sqrt{s}$) of 13 TeV collected by the ATLAS detector during the 2015–2018 data-taking periods after requiring stable LHC beams and that all detector subsystems were operational [43]. The primary luminosity measurement was performed using the LUCID-2 detector [44]. Candidate events are required to satisfy at least one of the dilepton triggers (ee, $\mu\mu$, $e\mu$) [41, 45, 46]. These triggers have looser identification and isolation requirements than the single-lepton triggers but have comparable signal efficiency for events satisfying the analysis selection. The lowest p_{T} threshold for the leading lepton range from 12 to 22 GeV and for the sub-leading lepton it ranged from 8 to 17 GeV.

To evaluate the effects of the detector resolution and acceptance on the signal and background, and to estimate the SM backgrounds, simulated event samples were produced using dedicated event generators. The detector response to the final-state particles was then modelled using a GEANT4-based Monte Carlo (MC) detector simulation [47, 48]. The simulated data must account for the fact that significantly more than one inelastic pp collision occurs per bunch crossing, with the average number ranging from 13 to 38 for the 2015–2018 data-taking periods, respectively. Inelastic collisions were simulated using PYTHIA 8.186 [49] with the A3 set of tuned parameters [50] and the NNPDF2.3LO [51] set of parton distribution functions (PDFs), and overlaid on the signal and background MC samples. These simulated events were reweighted to match the conditions of the collision data, specifically the number of additional pp interactions (pileup).

In order to optimize the signal selection and to estimate its acceptance and efficiency, a simulated VLL sample was generated using the model described in refs. [32, 33]. This model was implemented at LO, using MADGRAPH5_AMC@NLO 2.6.2 [52] with the NNPDF2.3LO PDF to generate the parton-level process, and selecting events with two, three, or four-or-more light leptons (ℓ) and ≥ 0 hadronically decaying τ-leptons, with all leptons having $p_{\text{T}} > 18$ GeV and $|\eta| < 2.8$. The generated τ' mass points are 130 GeV and 200 to 1300 GeV in steps of 100 GeV. These samples were then reweighted to next-to-leading order (NLO) in QCD. To perform the fragmentation and hadronization, these events were processed using PYTHIA 8.212 with the A14 set of tuned parameters [50] and the NNPDF2.3LO PDFs.

Since each VLL decays into a τ-lepton and either a vector boson or a Higgs boson, the selection requirements are ≥ 2 light leptons and ≥ 0 τ-leptons decaying to hadrons (τ_{had}). The leptonic decays of τ-leptons are not explicitly considered in the analysis. Top quark and multi-vector-boson events can contribute to the background since they have similar final states. Therefore, to estimate the SM backgrounds, samples of simulated events were generated, containing multiple final-state leptons that result from the decays of either directly produced vector bosons or vector bosons from top quark or H decays. Backgrounds from misidentified leptons are estimated with data-driven methods, as discussed in section 6.

The vector-boson samples were produced using either SHERPA 2.2.1 or SHERPA 2.2.2 [53] with the NNPDF3.0NNLO [54] set of PDFs, and the set of tuned parton-shower parameters developed by the authors of SHERPA [55]. The $V+$jets samples, where V is either a W or Z boson, and the semileptonic diboson samples were produced using SHERPA 2.2.1, while the fully leptonic diboson samples and the triboson samples were produced using SHERPA 2.2.2. The matrix element (ME) calculations were matched and merged with the SHERPA parton shower using the MEPS@NLO prescription [56–59] based on the Catani-Seymour dipole factorization procedure [60]. For the $V+$jets samples, the calculation was performed at NLO in QCD for up to two partons and at LO for up to four partons using the COMIX [61] and OPENLOOPS [62–64] libraries. For the diboson sample, this was performed for one parton at NLO and up to three partons at LO, while, for the triboson sample, the calculation was performed at NLO for the inclusive sample and at LO for up to two partons.

The electroweak production of single-top events, and also $t\bar{t}$ and $t\bar{t}+H$ production, was simulated by POWHEG BOX v2 [65–67] at NLO with the h_{damp} parameter[2] set to $1.5\,\mathrm{m_{top}}$ [68], the NNPDF3.0NLO [54] PDF set, and the top-quark mass set to 172.5 GeV. The diagram removal scheme [69] was employed to handle interference between single-top $t+W$ associated production and $t\bar{t}$ production [68]. Partons were hadronized and showered by PYTHIA 8.230 [70], using the A14 tune and the NNPDF2.3LO PDF set.

The $t\bar{t}+V$, $t+Z$, $t+WZ$, ttt, $t\bar{t}t\bar{t}$ and $t\bar{t}+WW$ events were generated by MADGRAPH5_aMC@NLO 2.3.3 [52] at NLO, using the NNPDF3.0NLO PDF set for $t\bar{t}+V$, $t+Z$, $t+WZ$, ttt and $t\bar{t}+WW$, and the NNPDF3.1NLO PDF set for $t\bar{t}t\bar{t}$. Parton hadronization and showering was performed by PYTHIA 8.210 using the A14 tune and the NNPDF2.3LO PDF set. A summary of simulated signal and background samples is provided in table 1.

4 Object reconstruction

All events used in this analysis are required to contain a primary vertex [71]. It is selected as the pp collision vertex candidate with the highest sum of the squared transverse momenta of all associated tracks with $p_{\mathrm{T}} > 500\,\mathrm{MeV}$. In addition, there must be at least two tracks associated with that vertex.

Electron candidates are reconstructed from energy clusters in the EM calorimeter that match a reconstructed track [72]. They are required to have $p_{\mathrm{T}} > 30\,\mathrm{GeV}$ in order to suppress the number of fake electrons. In addition, they are required to be within $|\eta| < 2.47$ with the region $1.37 < |\eta| < 1.52$ being excluded since it contains a significant amount of non-sensitive material in front of the calorimeter. To match these objects to the primary vertex, the track's transverse and longitudinal impact parameters (d_0 and z_0, respectively) are required to satisfy $|d_0|/\sigma(d_0) < 5$ and $|z_0 \sin\theta| < 0.5\,\mathrm{mm}$. Furthermore, through the application of one of several working points, these candidates must satisfy object identification criteria [72]. Each working point offers a trade-off between identification

[2]The h_{damp} parameter is a resummation damping factor and one of the parameters that controls the matching of POWHEG matrix elements to the parton shower. It effectively regulates the high-p_{T} radiation against which the $t\bar{t}$ system recoils.

JHEP07(2023)118

Process	ME Generator	ME Order	Showering Model	PDF
Signal	MadGraph5_aMC@NLO	LO	Pythia 8	NNPDF2.3lo
$Z \to \ell^+\ell^-$	Sherpa 2.2.1	NNLO	Sherpa	NNPDF3.0nnlo
$W \to \ell\nu_\ell$	Sherpa 2.2.1	NNLO	Sherpa	NNPDF3.0nnlo
VV (lep)	Sherpa 2.2.2	NLO	Sherpa	NNPDF3.0nnlo
VV (semi-lep)	Sherpa 2.2.1	NLO	Sherpa	NNPDF3.0nnlo
VVV	Sherpa 2.2.2	NLO	Sherpa	NNPDF3.0nnlo
t	Powheg Box v2	NLO	Pythia 8	NNPDF2.3lo
$t\bar{t}$	Powheg Box v2	NLO	Pythia 8	NNPDF2.3lo
$t\bar{t}+WW$	MadGraph5_aMC@NLO	NLO	Pythia 8	NNPDF2.3lo
$t\bar{t}+H$	Powheg Box v2	NLO	Pythia 8	NNPDF2.3lo
$t\bar{t}+V$	MadGraph5_aMC@NLO	NLO	Pythia 8	NNPDF2.3lo
ttt	MadGraph5_aMC@NLO	NLO	Pythia 8	NNPDF2.3lo
$t\bar{t}t\bar{t}$	MadGraph5_aMC@NLO	NLO	Pythia 8	NNPDF2.3lo
$t+Z$	MadGraph5_aMC@NLO	NLO	Pythia 8	NNPDF2.3lo
$t+WZ$	MadGraph5_aMC@NLO	NLO	Pythia 8	NNPDF2.3lo

Table 1. Simulated signal and background samples used in this analysis. The physics process is listed, along with the ME generator and order of the ME calculation, the parton hadronization and showering model, and the PDF used to simulate the process.

efficiency and misidentification rate. A likelihood-based discriminant is constructed from a set of variables that enhance electron selection, while rejecting photon conversions and hadrons misidentified as electrons [72]. An η- and E_{T}-dependent selection is applied to the likelihood discriminant in order to define specific working points. For this search, the *Tight* likelihood working point is used, which has a 75% efficiency at $E_{\mathrm{T}} = 30\,\mathrm{GeV}$, increasing to 88% at $E_{\mathrm{T}} = 100\,\mathrm{GeV}$ [72], when used to identify electrons from Z-boson decays. Electrons are also required to be isolated using criteria based on ID tracks and topological clusters in the calorimeter; the *Loose* isolation working point is applied and has an efficiency of approximately 99% [72]. Correction factors are applied to simulated electrons to take into account the small differences in reconstruction, identification and isolation efficiencies between data and MC simulation.

Muon candidates are reconstructed by combining a reconstructed track from the ID with one from the muon spectrometer [73], with the requirement that $p_{\mathrm{T}} > 20\,\mathrm{GeV}$ and $|\eta| < 2.5$. In addition, the transverse and longitudinal impact parameters of the track are required to satisfy $|d_0|/\sigma(d_0) < 3$ and $|z_0 \sin\theta| < 0.5\,\mathrm{mm}$. To reject misidentified muon candidates, primarily originating from pion and kaon decays, several quality requirements are imposed on the muon candidate. The *Medium* working point is used to select muons with $p_{\mathrm{T}} < 300\,\mathrm{GeV}$ and the *HighPt* working point is used for those with $p_{\mathrm{T}} > 300\,\mathrm{GeV}$ [73]. This choice ensures a 97% efficiency at $p_{\mathrm{T}} = 30\,\mathrm{GeV}$ for the *Medium* working point, and 76% at $p_{\mathrm{T}} = 500\,\mathrm{GeV}$ for the *HighPt* working point [73]. An isolation requirement based on ID tracks and topological clusters in the calorimeter is imposed. The *TightTrackOnly* isolation working point is used, resulting in an efficiency between 94% and 99% for muons from

JHEP07(2023)118

W-boson decays in simulated $t\bar{t}$ events [73]. Similarly to electrons, correction factors are applied to simulated muons to account for the small differences between data and simulation.

Particle-flow (PFlow) jets within $|\eta| < 4.5$ are reconstructed using the anti-k_t algorithm [74, 75] with a radius parameter $R = 0.4$ [76], using neutral PFlow constituents and charged constituents associated with the primary vertex as input [77]. These jets are then calibrated to the particle level by applying a jet energy scale derived from simulation [78]. Furthermore, in situ corrections based on the collected data are applied [78]. A cleaning procedure is used to identify and remove jets arising from calorimeter noise or non-collision backgrounds. To suppress jets arising from pileup, a discriminant called the "jet vertex tagger" (JVT) is constructed using a two-dimensional likelihood method [79]. The *Medium* JVT working point is used, which has an average efficiency of 95%. Jets used in this analysis are required to have $p_{\mathrm{T}} > 20\,\mathrm{GeV}$ and $|\eta| < 2.5$. Jets originating from b-quarks are identified using the DL1r b-tagging algorithm [80, 81]. The working point used corresponds to a b-tagging efficiency of 77% [80, 81], measured in a sample of simulated $t\bar{t}$ events. The corresponding rejection factors are approximately 130, 5, and 14 for light-quark and gluon jets, c-jets, and hadronically decaying τ-leptons, respectively. Correction factors are applied to the simulated jets to take account of the small differences in reconstruction and identification efficiencies, and the energy scale and resolution differences, between data and MC simulation.

The event selection for this analysis considers only those τ-leptons that decay into final states containing a ν_τ-neutrino and one-or-more hadrons, denoted by τ_{had}. Since the ν_τ escapes the detector volume undetected, only the hadronic decay products consisting of one or three charged hadrons and up to two neutral pions are visible and they are denoted by $\tau_{\text{had-vis}}$. Reconstruction of $\tau_{\text{had-vis}}$ [82, 83] is seeded by jets reconstructed from topological clusters by the anti-k_t algorithm with the radius parameter R set to 0.4. The tracks associated with the jet are required to originate from the primary vertex by satisfying the impact parameter requirements $|d_0| < 1\,\mathrm{mm}$ and $|z_0 \sin\theta| < 1.5\,\mathrm{mm}$. If these requirements are satisfied, the tracks are then required to be within a cone of size $\Delta R = 0.2$ around the jet axis, surrounded by a conical isolation region covering $0.2 < \Delta R < 0.4$, in order to be considered a $\tau_{\text{had-vis}}$ candidate. The direction of the $\tau_{\text{had-vis}}$ candidate in (η, ϕ) is calculated as the vector sum of the topological clusters within $\Delta R = 0.2$ of the jet axis, using the $\tau_{\text{had-vis}}$ vertex as the origin. A multivariate discriminant is used to select tracks that were produced by charged τ_{had} decay products [82, 83]. Reconstructed $\tau_{\text{had-vis}}$ objects are selected for the analysis if they have exactly one or three associated tracks (1- or 3-prong) with a total charge equal to ± 1. The $\tau_{\text{had-vis}}$ objects must also satisfy the requirements $p_{\mathrm{T}} > 20\,\mathrm{GeV}$ and $|\eta| < 2.47$, excluding the region $1.37 < |\eta| < 1.52$. These requirements have an efficiency of about 85% for 1-prong and 70% for 3-prong $\tau_{\text{had-vis}}$ objects [82, 83] as estimated from simulated $Z/\gamma^* \to \tau^+\tau^-$ events. A multivariate regression technique trained on MC samples is used to determine the $\tau_{\text{had-vis}}$ energy scale using information from associated tracks, calorimeter energy clusters, and reconstructed neutral pions [82, 83].

A recurrent neural network (RNN) classifier [84] is employed to select τ_{had}-initiated jets and reject those initiated by quarks or gluons. The RNN is trained on simulated $Z/\gamma^* \to \tau^+\tau^-$ (for signal) and simulated dijet events (for background). The training

	Electrons		Muons		$\tau_{\text{had-vis}}$
	Tight likelihood	*Loose* isolation	*Medium* (*HighPt*)	*TightTrackOnly* isolation	*Medium* RNN
Tight	Pass	Pass	Pass	Pass	Pass
Loose	Fail*	Fail*	Pass	Fail	Fail

*Loose electrons are defined as failing either the *Tight* likelihood or the *Loose* isolation requirements, but not both.

Table 2. Object definitions used in the analysis for leptons. Tight objects are those selected for the nominal analysis and pass the prescribed selection requirements. Loose objects are those used to assess the contribution from the fake-lepton background and fail one or more selection requirements.

variables are single-track variables, and reconstructed kinematic and topological variables. This analysis uses the *Medium* working point with an efficiency of 75% (60%) for 1-prong (3-prong) candidates and a background rejection factor of 35 (240). A boosted decision tree [82, 83] is used to reject electron backgrounds misidentified as 1-prong $\tau_{\text{had-vis}}$ objects. Variables used for its training include information from the calorimeter, the tracking detector, and the visible momentum measured from the reconstructed tracks. The *Tight* working point with an efficiency of 75% is used. To assess the contribution from misidentified leptons (section 6), less stringent (Loose) object identification requirements are applied. When selecting Loose $\tau_{\text{had-vis}}$ there is an additional requirement for the RNN score to be at least 0.01. In addition, a dedicated muon-veto criterion is used to reject muons reconstructed as $\tau_{\text{had-vis}}$. Correction factors are applied to simulated τ_{had} objects to take into account the small differences in reconstruction and identification efficiencies between data and MC simulation. The energy scale and resolution differences between data and MC simulation are also accounted for by applying scale factors. A summary of the lepton object definitions is presented in table 2.

The missing transverse momentum (with magnitude $E_{\text{T}}^{\text{miss}}$) [85] is reconstructed as the negative vector sum of the p_{T} of all the selected electrons, muons, jets, and $\tau_{\text{had-vis}}$. An extra track-based "soft term" is built using additional tracks associated with the primary vertex, but not with any reconstructed object. The use of this track-based soft term is motivated by improved performance in $E_{\text{T}}^{\text{miss}}$ in a high pileup environment.

To avoid cases where the detector response to a single physical object is reconstructed as two separate final-state objects, an overlap removal procedure is used. If electron and muon candidates share a track, the electron candidate is removed. After that, if the $\Delta R_{y,\phi}$ distance[3] between a jet and an electron candidate is less than 0.2, the jet is discarded. If multiple jets satisfy this requirement, only the closest jet is removed. For jet-electron distances between 0.2 and 0.4, the electron candidate is removed. If the distance between a jet and a muon candidate is less than 0.4, the muon candidate is removed if the jet has more than two associated tracks; otherwise the jet is removed. The τ_{had} candidates are seeded from jets, so this procedure removes any ambiguity in their selection.

[3] $\Delta R_{y,\phi}$ is the Lorentz-invariant distance in the rapidity-azimuthal-angle plane, defined as $\Delta R_{y,\phi} = \sqrt{(\Delta y)^2 + (\Delta\phi)^2}$ where the rapidity is $y = (1/2)[(E + p_z)/(E - p_z)]$.

Variables	BDT Training Regions						
BDT	2ℓ SSSF, 1τ	2ℓ SSOF, 1τ	2ℓ OSSF, 1τ	2ℓ OSOF, 1τ	2ℓ, $\geq 2\tau$	3ℓ, $\geq 1\tau$	4ℓ, $\geq 0\tau$
N_ℓ	2	2	2	2	2	3	≥ 4
Charge/flavour	SSSF	SSOF	OSSF	OSOF	—	—	—
N_τ	1	1	1	1	≥ 2	≥ 1	≥ 0
$E_{\mathrm{T}}^{\mathrm{miss}}$ [GeV]	≥ 120	≥ 90	≥ 60	≥ 100	≥ 60	≥ 90	≥ 60

Table 3. The regions used in the training and optimization of the BDT. The training regions are split according to the number of light leptons (N_ℓ), and their charge (SS same charge, OS opposite charge) and flavour (SF same flavour, OF opposite flavour), the number of τ_{had} (N_τ), and the missing transverse momentum ($E_{\mathrm{T}}^{\mathrm{miss}}$). Every region has a requirement that it contain at least one jet ($N_{\mathrm{jet}} > 0$).

Variables	Signal Regions						
BDT	2ℓ SSSF, 1τ	2ℓ SSOF, 1τ	2ℓ OSSF, 1τ	2ℓ OSOF, 1τ	2ℓ, $\geq 2\tau$	3ℓ, $\geq 1\tau$	4ℓ, $\geq 0\tau$
BDT Score	≥ 0.15	≥ 0.1	≥ 0.1	≥ 0.1	≥ -0.11	≥ 0.08	≥ 0.08

Table 4. The BDT score requirement imposed on the training regions that are used to define the signal regions. No other requirement differs between the two regions.

5 Analysis strategy

Based on the production and decay modes of the τ' and ν_τ' given in section 1, the multilepton final states are expected to maximize the signal sensitivity, and hence the multilepton final states are used to search for the VLL signal. To further optimize the signal sensitivity, the different decay modes are targeted by splitting the data into seven training regions (given in table 3) based on the numbers of light leptons and τ_{had}, and a $E_{\mathrm{T}}^{\mathrm{miss}}$ requirement. In all regions at least one jet is required. Additional requirements are derived by maximizing the signal significance through the application of a BDT [36, 37]. This leads to the seven signal regions (SRs) defined in table 4.

In addition to the seven SRs, three control regions (CRs) are used in order to normalize the dominant physics background ($t\bar{t} + Z$, WZ, and ZZ) estimates to data, and a fourth CR is used to assess fake τ_{had} objects originating from gluon-initiated jets and pileup. These CRs are defined in table 5. Since events in the WZ CR do not have a τ-lepton, its kinematic variables are set to zero when calculating the BDT score. To confirm that the CRs are modelled correctly and that the obtained background normalization factors are also valid in the regions with different numbers of light leptons and τ-leptons, three validation regions (VRs) are defined, as also shown in table 5. An additional seven VRs are used to confirm that the BDT models the data correctly. These VRs are selected where the BDT distribution is expected to primarily contain background events, as shown in figure 5. The SRs, CRs, and VRs are selected such that there is no overlap of events between the regions. The BDT distribution shape in the CRs is shown in figure 2, which demonstrates good agreement between data and the background simulation.

JHEP07(2023)118

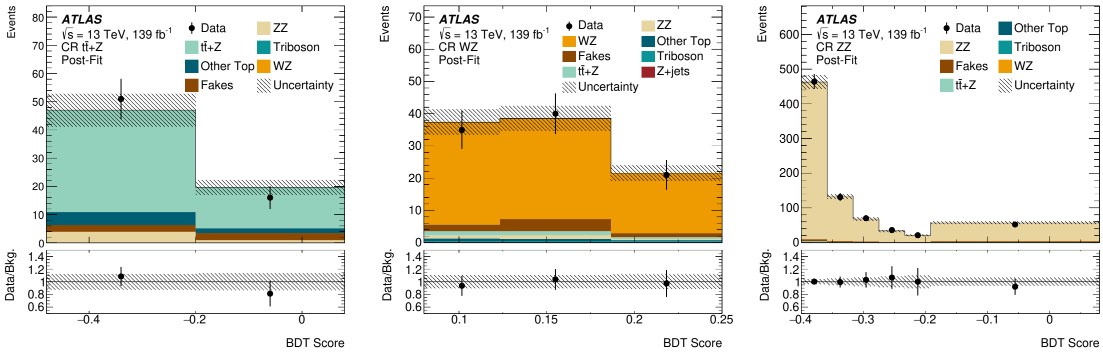

(a) (b) (c)

Figure 2. A comparison of the BDT scores for data and the predicted background after performing the fit described in section 8 in the CRs used to estimate the three dominant backgrounds: (a) $t\bar{t}+Z$, (b) WZ, and (c) ZZ. The first bin of the $t\bar{t}+Z$ and ZZ distributions contains underflow events, while the last bin of the WZ distribution contains overflow events. The hatched band represents the combined statistical and systematic uncertainties.

	Control Regions				Validation Regions		
	$t\bar{t}+Z$	WZ	ZZ	Fake τ_{had}	$t\bar{t}+Z$	WZ	ZZ
BDT	4ℓ, $\geq 0\tau$	3ℓ, $\geq 1\tau$	4ℓ, $\geq 0\tau$	2ℓ OSSF, 1τ	3ℓ, $\geq 1\tau$	2ℓ SSOF, 1τ	3ℓ, $\geq 1\tau$
N_ℓ	≥ 4	3	≥ 4	2	3	2	3
N_τ	≥ 0	0	≥ 0	1	≥ 1	1	≥ 1
N_b	> 0	0	0	—	> 0	0	0
$E_{\text{T}}^{\text{miss}}$ [GeV]	≥ 60	≥ 90	< 60	≥ 60	—	—	—
Charge/flavour	—	—	—	OSSF	—	SSOF	—
BDT score	< 0.08	≥ 0.08	< 0.08	< -0.15	< 0.08	< 0.1	< 0.08

Table 5. The definition of the CRs used to determine the normalization of the largest backgrounds, as well as the CR used to assess fake τ-leptons originating from gluon-initiated jets and pileup. In addition, the VRs used to validate the CRs are also defined. Both the CRs and VRs are selected so that they do not overlap with the SRs or with each other, but are similar enough to avoid problems when extrapolating between the regions. Like the SRs, the CRs and VRs have the requirement that $N_{\text{jet}} > 0$. A dash indicates that the variable is not used for the corresponding CR or VR.

To classify the events as signal or background, the AdaBoost BDT algorithm [36, 37] is used as implemented in the scikit-learn package [86]. The training and optimization of the BDT are performed in two steps. The first step is the optimization of the BDT hyperparameters and the second step is the optimization of the training through the selection of the variables used for the training.

To optimize the hyperparameters (maximum tree depth, maximum features per split, minimum samples per leaf, minimum samples per split, number of estimators, and learning rate) the set of 34 kinematic and topological variables listed in table 6 were used. These variables are chosen as they are expected to provide good separation between the background and signal topologies. To avoid biasing the search by selecting a specific mass, the simulated signal samples described in section 3 are combined with equal weight for $M_{\tau'}$ set to 800 GeV, 900 GeV and 1000 GeV to train the BDT. All of the background samples are considered in the training, including all fake leptons. A scan over the hyperparameters is performed using the 5-fold cross-validation procedure to train the BDT, where the simulated data samples are split into five equal randomized samples, with four being used in the training and the fifth used as a testing sample. The training is performed five times so that each of the five samples is used as a testing sample. The set of hyperparameters with the highest receiver operating characteristic (ROC) score is selected.

To select the optimal set of training variables, a BDT is trained in each analysis region defined by lepton multiplicity using the full set of 34 variables. The ranking of the variables is evaluated using the procedure provided by the scikit-learn package. The lowest-ranked training variable is then removed and the BDT is retrained. This procedure is repeated until the ROC score decreases by more than 1%. This leads to each SR having its own unique set of training variables, which are listed in table 7.

The final training variables are individually compared with data to confirm that they are well modelled. To avoid any bias in the analysis, only events with a BDT score not satisfying the SR criteria (table 4) are used in the comparison, since they are background dominated. Through the use of a χ^2 test, a probability of $> 5\%$ is found for agreement between data and simulation for all variables used in the BDT training. Figure 3 shows the distributions of some highly ranked variables in each of the BDT training regions.

6 Background estimation

There are two basic categories of backgrounds to the signal. One category, the irreducible backgrounds, is defined by those processes that yield the same final state as the signal. The other category, the reducible backgrounds, is defined by those that mimic the final state because of misidentified leptons or non-prompt leptons as well as misidentified lepton charge. The irreducible backgrounds are estimated from the simulated samples discussed in section 3.

Similarly to ref. [87] the simulated background in the WZ CR is found not to agree with data when examined as a function of the number of jets in the event. Since inverting the BDT score criteria for this CR yielded a similar mismodelling, the data in this region are used to calculate a scale factor to correct the MC simulation to the data in the WZ CR, which then agreed with data.

Charge misidentification for electrons arises from photon conversions or bremsstrahlung, and its rate is challenging to describe through detector simulation. Therefore, scale factors are derived and applied to simulated background events to match the charge misidentification probabilities observed in data. The scale factors are derived using a $Z \to e^+e^-$ data sample and are parameterized as a function of p_{T} and η [72].

The reducible backgrounds from misidentified leptons (electron, muons and τ_{had}) are estimated from data by using the fake-factor (FF) method to derive a transfer function from a background-dominated region to the SR [88]. The transfer function is the ratio of events passing a tight lepton selection to events passing a loose lepton selection in the

JHEP07(2023)118

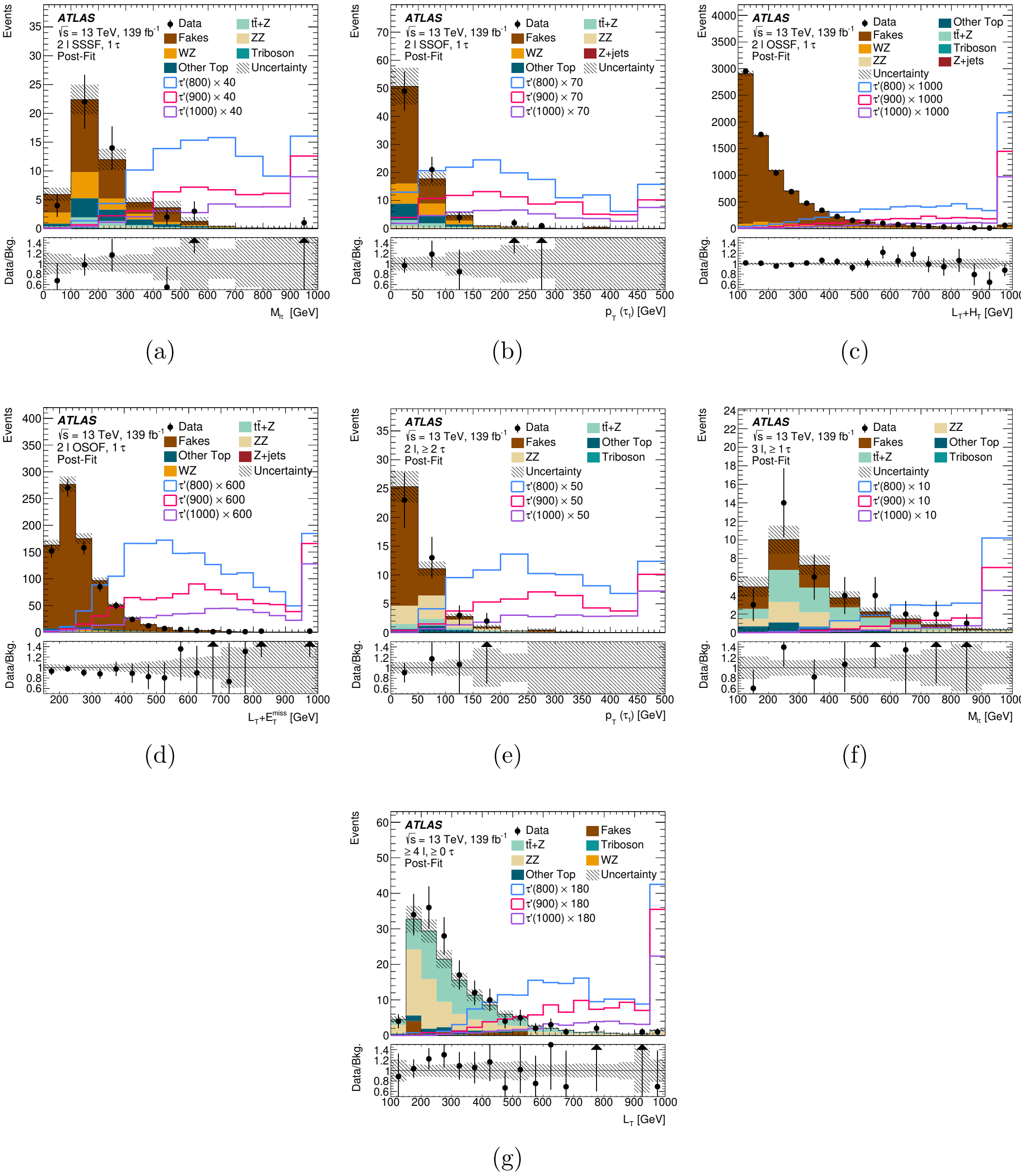

Figure 3. A comparison of the total background and signal distributions for $M_{\tau'} = 800$, 900 and 1000 GeV in variables that are highly ranked in the BDT training. The signal distribution is scaled by the value indicated in the legend. The background prediction is taken after performing the fit described in section 8, while the signal prediction is taken before the fit. The hatched band represents the combined statistical and systematic uncertainties. The last bin contains overflow events. The arrows in the ratio plot are for points that are outside the range. (a) $M_{\ell\tau}$ for the 2 ℓ SSSF, 1 τ training region (b) $p_{\mathrm{T}}(\tau_1)$ for the 2 ℓ SSOF, 1 τ training region (c) $L_{\mathrm{T}} + H_{\mathrm{T}}$ for the 2 ℓ OSSF, 1 τ training region (d) $L_{\mathrm{T}} + E_{\mathrm{T}}^{\mathrm{miss}}$ for the 2 ℓ OSOF, 1 τ training region (e) $p_{\mathrm{T}}(\tau_1)$ for the 2 ℓ, ≥ 2 τ training region (f) $M_{\ell\tau}$ for the 3 ℓ, ≥ 1 τ training region (g) L_{T} for the ≥ 4 ℓ, ≥ 0 τ training region.

JHEP07(2023)118

Variable	Description
$E_{\mathrm{T}}^{\mathrm{miss}}$	The missing transverse momentum in the event
$\mathcal{S}(E_{\mathrm{T}}^{\mathrm{miss}})$	The missing transverse momentum's significance in the event
L_{T}	The scalar sum of light lepton p_{T} in the event
$L_{\mathrm{T}} + E_{\mathrm{T}}^{\mathrm{miss}}$	The scalar sum of light lepton p_{T} and the missing transverse momentum in the event
$L_{\mathrm{T}} + p_{\mathrm{T}}(\tau)$	The scalar sum of light lepton p_{T} and τ-lepton p_{T} in the event
$p_{\mathrm{T}}(\ell_1)$	The leading light lepton's p_{T} in the event
$p_{\mathrm{T}}(\ell_2)$	The sub-leading light lepton's p_{T} in the event
$p_{\mathrm{T}}(j_1)$	The leading jet's p_{T} in the event
$p_{\mathrm{T}}(\tau_1)$	The leading τ-lepton's p_{T} in the event
N_j	The number of jets in the event
N_b	The number of b-jets in the event
H_{T}	The scalar sum of jet p_{T} in the event
$L_{\mathrm{T}} + H_{\mathrm{T}}$	The scalar sum of light lepton p_{T} and jet p_{T} in the event
$M_{\ell\ell}$	The invariant mass of all light leptons in the event
$M_{\ell\tau}$	The invariant mass of all light leptons and τ-leptons in the event
$M_{\ell j}$	The invariant mass of all light leptons and jets in the event
M_{jj}	The invariant mass of all jets in the event
$M_{j\tau}$	The invariant mass of all jets and τ-leptons in the event
M_{T}	The transverse mass of the leading light lepton and $E_{\mathrm{T}}^{\mathrm{miss}}$ in the event
M_{OSSF}	The invariant mass of the opposite-sign same-flavour light-lepton pair closest to the Z mass in the event
$\Delta\phi(j_1 E_{\mathrm{T}}^{\mathrm{miss}})$	$\Delta\phi$ between the leading p_{T} jet in the event and $E_{\mathrm{T}}^{\mathrm{miss}}$
$\Delta\phi(\ell_1 E_{\mathrm{T}}^{\mathrm{miss}})$	$\Delta\phi$ between the leading p_{T} light lepton in the event and $E_{\mathrm{T}}^{\mathrm{miss}}$
$\Delta\phi(\ell_1 \ell_2)$	$\Delta\phi$ between the leading and sub-leading p_{T} light leptons in the event
$\Delta\phi(\ell_1 j_1)$	$\Delta\phi$ between the leading p_{T} light lepton and jet in the event
$\Delta\phi(\tau_1 E_{\mathrm{T}}^{\mathrm{miss}})$	$\Delta\phi$ between the leading p_{T} τ-lepton in the event and $E_{\mathrm{T}}^{\mathrm{miss}}$
$\Delta\phi(\ell_1 \tau_1)$	$\Delta\phi$ between the leading p_{T} light lepton and τ-lepton in the event
$\Delta\phi(j_1 \tau_1)$	$\Delta\phi$ between the leading p_{T} jet and τ-lepton in the event
$\Delta R(j_1 E_{\mathrm{T}}^{\mathrm{miss}})$	ΔR between the leading p_{T} jet in the event and $E_{\mathrm{T}}^{\mathrm{miss}}$
$\Delta R(\ell_1 E_{\mathrm{T}}^{\mathrm{miss}})$	ΔR between the leading p_{T} light lepton in the event and $E_{\mathrm{T}}^{\mathrm{miss}}$
$\Delta R(\ell_1 \ell_2)$	ΔR between the leading and sub-leading p_{T} light leptons in the event
$\Delta R(\ell_1 j_1)$	ΔR between the leading p_{T} light lepton and jet in the event
$\Delta R(\tau_1 E_{\mathrm{T}}^{\mathrm{miss}})$	ΔR between the leading p_{T} τ-lepton in the event and $E_{\mathrm{T}}^{\mathrm{miss}}$
$\Delta R(\ell_1 \tau_1)$	ΔR between the leading p_{T} light lepton and τ-lepton in the event
$\Delta R(j_1 \tau_1)$	ΔR between the leading p_{T} jet and τ-lepton in the event

Table 6. List of the input variables used to train the BDT. The final set is reduced by assessing the impact of removing the lowest-ranked variables on the ROC score for each training region independently.

background-dominated CR. The FF is used to estimate the probability of an object being either a misidentified lepton or a non-prompt lepton from an in-flight decay. The FF is calculated as a function of the lepton p_{T}.

Non-prompt or fake light leptons can originate from decays of bottom or charm hadrons, pion or kaon decays, jets misidentified as electrons, and electrons from photon conversions. To calculate the transfer function for electrons, the background CR requires exactly one electron with a loose selection and no other leptons, $E_{\mathrm{T}}^{\mathrm{miss}} < 40\,\mathrm{GeV}$, $N_{\mathrm{jet}} \geq 2$, and no reconstructed b-jets. The background CR for muons requires exactly one muon with a loose selection and zero electrons and τ-leptons, $E_{\mathrm{T}}^{\mathrm{miss}} < 40\,\mathrm{GeV}$, and at least two jets with the leading jet $p_{\mathrm{T}} > 35\,\mathrm{GeV}$.

Since only τ_{had} decays are selected, misidentified τ-leptons originate from jets that can arise from several sources: light- and heavy-flavour jets, gluon radiation, and jets from

Variable	2ℓ SSSF, 1τ	2ℓ SSOF, 1τ	2ℓ OSSF, 1τ	2ℓ OSOF, 1τ	2ℓ, $\geq 2\tau$	3ℓ, $\geq 1\tau$	4ℓ, $\geq 0\tau$
$p_{\mathrm{T}}(\tau_1)$	1	1	1	1	2	2	
$M_{\ell\tau}$	2	2	5	3	1	1	
$L_{\mathrm{T}} + E_{\mathrm{T}}^{\mathrm{miss}}$	3	3	2	2	23	4	1
$E_{\mathrm{T}}^{\mathrm{miss}}$	4	7	4	21	5	8	5
$\Delta\phi(\tau_1 E_{\mathrm{T}}^{\mathrm{miss}})$	5	6	6	13	3	3	
$\Delta R(\ell_1 \ell_2)$	6	24	7	7	15		17
M_{jj}	7	21	24	15	1	12	19
$M_{\ell j}$	8	11	26	11	27	14	2
$\Delta\phi(\ell_1 E_{\mathrm{T}}^{\mathrm{miss}})$	9	16	20	8	20	10	15
$\Delta R(\ell_1 \tau_1)$	10	8	12	6	16	15	
$\Delta R(j_1 \tau_1)$	11	9	17	25	25	23	
$\Delta R(\ell_1 E_{\mathrm{T}}^{\mathrm{miss}})$	12	29	11	19	17	11	10
$\Delta\phi(\ell_1 \ell_2)$	13	13	18	16	28	13	9
$\Delta R(\tau_1 E_{\mathrm{T}}^{\mathrm{miss}})$	14	27	9	5	12	9	
$p_{\mathrm{T}}(j_1)$	15	19	10	12	22	19	11
M_{T}	16	23	16	18	8	17	7
$\Delta\phi(j_1 \tau_1)$	17	20	27	29	24		
$M_{\ell\ell}$	18	10	25	20	10	22	4
$p_{\mathrm{T}}(\ell_1)$	19	4			30	5	16
$\mathcal{S}(E_{\mathrm{T}}^{\mathrm{miss}})$	20	5	14	24	9	24	8
N_j	21	14	28	23	26		22
$L_{\mathrm{T}} + p_{\mathrm{T}}(\tau)$	22	22		26			
$p_{\mathrm{T}}(\ell_2)$	23	15			18		
$\Delta R(j_1 E_{\mathrm{T}}^{\mathrm{miss}})$	24	18	23	10	31		21
$\Delta\phi(\ell_1 j_1)$	25	17	13	17	13	25	13
N_b	26	26	21	22	29	20	14
L_{T}	27	32			32		3
$M_{j\tau}$	28	31	15	9	6	18	
$\Delta R(\ell_1 j_1)$	29		8	4	11		18
$L_{\mathrm{T}} + H_{\mathrm{T}}$		12	3	14			
M_{OSSF}			22		7	6	12
$\Delta\phi(\ell_1 \tau_1)$		25	19		19	16	
$\Delta\phi(j_1 E_{\mathrm{T}}^{\mathrm{miss}})$				27	21		6
H_{T}		28		28	33	21	20

Table 7. The ranking of the variables used as inputs to the BDT algorithm for each of the training regions. Variables are ranked relative to each other by counting the instances a particular variable is used by the BDT nodes in defining the signal-background separation. Variables that do not have a ranking are not included in the corresponding training region. The final variables in each training region are selected using an optimization procedure.

pileup. The SRs are dominated by light- and heavy-flavour jets misidentified as τ-leptons. Therefore, FFs are calculated independently in dedicated CRs corresponding to light- and heavy-flavour jets. The $Z+$jets FF CR uses a $Z+$jets sample, which is enriched in light-flavour fake τ-leptons with a requirement of $Z \to \mu^+\mu^-$ decay and $|m_{\mu\mu} - m_Z| < 15\,\text{GeV}$. In addition, the sample is required to have zero reconstructed b-jets and $E_{\text{T}}^{\text{miss}} < 60\,\text{GeV}$. The $t\bar{t}$ FF CR is a dilepton $t\bar{t}$ sample, enriched in heavy-flavour fake τ-leptons with a requirement of exactly two light leptons that satisfy $|m_{\ell\ell} - m_Z| > 10\,\text{GeV}$, exactly one τ-lepton that satisfies the loose criteria, and at least two jets with at least one satisfying the b-jet requirements. The FF is calculated separately for 1- and 3-prong τ-leptons. The FFs calculated in the $Z+$jets and $t\bar{t}$ CRs are combined by performing a template fit of the BDT score in each training region. The fit uses MC "truth"-matched fake τ-leptons to compare the fake composition in the analysis region and the $Z+$jets and $t\bar{t}$ CRs. The modelling of the background originating from fake leptons is verified by performing closure tests in the regions where the FFs are derived as well as by comparing the background estimates to data in the VRs.

7 Systematic uncertainties

The systematic uncertainties considered in this analysis come from instrumental and theoretical sources, affecting both the overall event yield and the shape of the distribution. They are evaluated by varying each source around its nominal value as described below.

The uncertainties in the theoretical production cross sections used to simulate the background events are calculated following the same approach as in ref. [89]. These uncertainties are assigned to every background process whose normalization is not determined by the fit. These backgrounds come from $Z+$jets, WW, triple vector boson, and top-quark processes (excluding $t\bar{t}+Z$).

Uncertainties from missing higher-order contributions are evaluated [90] by applying seven independent variations of the QCD factorization and renormalization scales by factors of one-half and two in the matrix elements after removing combinations that differ by a factor of four. The effect of the uncertainty in the strong coupling constant $\alpha_{\text{s}}(m_Z) = 0.118$ as well as the uncertainties in the nominal PDF set, used in the generation of simulated events, is evaluated by following the PDF4LHC recommendations [91]. In addition, the modelling uncertainty due to the choice of generator for $t\bar{t}+Z$ production is evaluated by comparing samples from the nominal generator MC@NLO + Pythia 8 and the alternative generator Sherpa 2.2.1. This gives an uncertainty of up to 7.9% in the $t\bar{t}+Z$ background estimate.

The uncertainty in the full integrated luminosity as obtained from the LUCID-2 detector is 1.7% [44] and is applied to the background and signal processes that are normalized to the theoretical predictions. Uncertainties associated with the pileup reweighting procedure range from 0.2% to 3.5% [92].

Instrumental uncertainties are evaluated for each object that is considered in the analysis. For the selected leptons, they originate from the reconstruction and identification efficiency, the energy (momentum) scale and resolution, and the isolation efficiency [72, 73, 93]. The uncertainty related to trigger efficiencies is also included. For jets, the uncertainties

JHEP07(2023)118

originate from the jet energy scale and resolution [77, 94], the matching of jets to the primary vertex [92], and the identification of b-jets [80, 81]. Furthermore, the impact of a possible miscalibration of the soft-track component of the $E_{\mathrm{T}}^{\mathrm{miss}}$ is derived from a data-MC comparison of the p_{T} balance of the hard and soft $E_{\mathrm{T}}^{\mathrm{miss}}$ components [95].

Systematic uncertainties associated with the light-lepton FFs [88] account for the jet composition differences between the region where the FFs are derived and the analysis regions where they are applied, as well as the differences between the values of FFs calculated in regions with different selection requirements. Additionally, the uncertainty arising from the modelling and limited sample sizes is taken into account. The uncertainties are treated independently for each of the different sources of misidentified objects.

Uncertainties from several sources are evaluated for the FF derived for τ-leptons. Most notably, to account for the limited numbers of simulated events in the regions used to determine the composition of fake τ-lepton samples, the uncertainty of the fitted fractions from the template fit to the $Z+$jets and $t\bar{t}$ FF CRs, is evaluated as the difference between the two values 0% and 100%, for each SR. Furthermore, a systematic uncertainty to account for the gluon- and pileup-initiated fake τ-lepton contribution is applied. To assess this uncertainty a new CR is defined with a less restrictive RNN score requirement on the loose $\tau_{\text{had-vis}}$ in the $Z+$jets FF CR, which increases this contribution from roughly 40% to 60% in the CR. The systematic uncertainty in the estimated number of fake τ-leptons is then taken as the difference between applying the nominal FF in each SR and the FF calculated with the less restrictive RNN requirement. The nominal FF is calculated by applying a minimum RNN requirement of 0.01, while for the assessment of its systematic uncertainty a minimum value of 0.005 is used. Since gluon- and pileup-initiated fake τ-leptons typically have low p_{T}, the τ-lepton FF systematic uncertainties are split into $<$40 GeV and $>$40 GeV regions and assessed independently. The gluon- and pileup-initiated contribution is only taken for fake τ-leptons with p_{T} less than 40 GeV, and the large uncertainty of 28% is constrained in the Fake τ_{had} CR (table 5), which is a highly populated region dominated by gluon- and pileup-initiated fake τ-leptons. However, the gluon- and pileup-initiated fake τ-lepton fraction is less than 20% in the SRs, where the BDTs tend to select τ-leptons with p_{T} greater than 40 GeV, so this uncertainty does not have an impact on them. Additionally, uncertainties are derived for the τ-lepton FFs by accounting for the numbers of events in the $Z+$jets and $t\bar{t}$ FF CRs.

8 Results

In order to test for the presence of a VLL signal, the BDT score templates for signal and background events are fitted to the data using a binned maximum-likelihood (ML) approach in the RooFit and RooStats frameworks [96, 97]. The normalizations to data of the main background component modelled in the CR templates (WZ, ZZ, $t\bar{t}+Z$), and SR VLL templates are allowed to vary without constraints. The other backgrounds' normalizations are assigned Gaussian constraints based on their normalization uncertainties. In addition, the systematic uncertainties are included in the fit as nuisance parameters with correlations across regions and processes taken into account. To quantify the statistical significance of

Signal Regions	$2\,\ell$ SSSF, $1\,\tau$	$2\,\ell$ SSOF, $1\,\tau$	$2\,\ell$ OSSF, $1\,\tau$	$2\,\ell$ OSOF, $1\,\tau$	$2\,\ell$, $\geq 2\,\tau$	$3\,\ell$, $\geq 1\,\tau$	$\geq 4\,\ell$, $\geq 0\,\tau$
Observed Events	6	3	37	7	4	2	8
Total Background	4.60 ± 0.60	3.70 ± 0.40	28.00 ± 1.80	3.80 ± 0.50	5.70 ± 0.40	3.90 ± 0.30	7.20 ± 0.70
Other Top	0.81 ± 0.19	0.85 ± 0.24	1.60 ± 0.40	0.63 ± 0.19	0.76 ± 0.09	0.35 ± 0.07	0.44 ± 0.13
$t\bar{t}+Z$	0.14 ± 0.04	0.28 ± 0.07	2.10 ± 0.40	0.08 ± 0.05	0.82 ± 0.16	1.11 ± 0.20	3.10 ± 0.60
ZZ	0.09 ± 0.02	0.13 ± 0.02	1.83 ± 0.14	0.05 ± 0.01	2.06 ± 0.28	1.10 ± 0.12	2.00 ± 0.25
WZ	0.95 ± 0.16	1.28 ± 0.19	12.40 ± 1.60	0.51 ± 0.09	< 0.01	< 0.01	0.06 ± 0.04
Triboson	0.14 ± 0.02	< 0.01	0.47 ± 0.04	< 0.01	0.05 ± 0.01	0.10 ± 0.01	0.19 ± 0.02
Fakes	2.40 ± 0.50	1.18 ± 0.17	9.60 ± 1.50	2.50 ± 0.40	2.03 ± 0.17	1.20 ± 0.13	1.39 ± 0.34
$\tau'(130\,\text{GeV})$*	3.40 ± 2.40	8.00 ± 4.00	11.00 ± 5.00	6.00 ± 2.40	25.00 ± 6.00	13.00 ± 4.00	5.40 ± 3.50
$\tau'(500\,\text{GeV})$*	12.60 ± 0.80	13.60 ± 0.80	29.60 ± 1.40	10.70 ± 0.70	13.80 ± 1.00	13.70 ± 0.70	4.70 ± 0.40
$\tau'(800\,\text{GeV})$*	2.35 ± 0.13	2.20 ± 0.12	6.16 ± 0.30	2.48 ± 0.14	1.72 ± 0.13	2.25 ± 0.13	0.94 ± 0.06
$\tau'(1000\,\text{GeV})$*	0.73 ± 0.04	0.67 ± 0.04	1.90 ± 0.09	0.82 ± 0.04	0.51 ± 0.04	0.68 ± 0.04	0.29 ± 0.02

*Pre-fit

Table 8. Total observed yields as computed by the fit for signal regions. The uncertainty contains both the systematic and statistical uncertainties. The prediction for each background sample is taken after a likelihood fit is performed to measure the VLL production cross section. Background normalization factors are also applied. The "Other Top" sample includes contributions from single top, $t\bar{t}$, $t\bar{t}+W$, $t+Z$, $t+WZ$, $t\bar{t}+H$, $t\bar{t}+WW$, $t\bar{t}t\bar{t}$, and ttt. The prediction from the signal samples is taken before the likelihood fit is performed. The background contributions may not add up to equal the total background due to rounding.

the fit and its resulting power to reject the background-only hypothesis, a test statistic is constructed using the profile likelihood ratio [98].

After performing the simultaneous fit of the seven SRs and four CRs to the data, the fitted normalization factors relative to the theoretical expectations for the main backgrounds are 1.06 ± 0.14 for WZ, 1.02 ± 0.07 for ZZ, and 1.18 ± 0.18 for $t\bar{t}+Z$. Figure 4 shows a comparison between the data and the signal and background yields for the SRs, CRs, and corresponding VRs. Figure 5 shows the templates and data versus BDT score for each of the analysis regions after applying the selection requirements in table 4 but before the SR's BDT requirement is applied. The regions with BDT score values less than the SR requirement are used as VRs. In all SRs the number of observed events is compatible with the background hypothesis. Tables 8 and 9 show the total background and signal yields in all SRs and CRs after fitting to data.

Table 10 shows the impact of each source of systematic uncertainty on the signal strength μ in the signal-plus-background fit. Signal strength is defined as the ratio of the signal cross section estimated using the data to the predicted signal cross section. The nuisance parameters are grouped according to their origin. To evaluate the impact of each source of systematic uncertainty, the source is removed from the full fit and the signal strength and its uncertainty are recalculated. The square of the impact is defined as the decrease in the squared signal-strength uncertainty. The nuisance parameters associated with the background normalization have the highest impact on μ, while the systematic uncertainties associated with the fake-lepton estimation have the second-highest impact.

Using the VLL doublet model in refs. [32, 33], the predicted significance of the signal is expected to be greater than 5 standard deviations for $M_{\tau'}$ in the range from 130 to 600 GeV and greater than 3 standard deviations for values of $M_{\tau'}$ up to 800 GeV. Above this mass

JHEP07(2023)118

Control Regions	$t\bar{t}$+Z	$W\ Z$	ZZ	Fake τ
Observed events	67	96	774	7743
Total background	67 ± 8	97 ± 9	774 ± 28	7760 ± 90
Z+jets	< 0.03	0.1 ± 0.1	< 0.03	2.55 ± 0.32
Other Top	6.3 ± 0.9	2.0 ± 0.6	0.73 ± 0.14	66 ± 7
$t\bar{t}$+Z	51 ± 8	3.1 ± 0.6	6.5 ± 1.2	52 ± 9
ZZ	4.8 ± 0.5	2.5 ± 0.2	753 ± 28	95 ± 5
WZ	10.0 ± 0.1	82 ± 9	0.17 ± 0.03	370 ± 50
Triboson	< 0.03	0.9 ± 0.1	0.44 ± 0.04	1.71 ± 0.15
Fakes	4.8 ± 0.8	7.0 ± 0.7	12.4 ± 1.2	7170 ± 100
τ'(130 GeV)*	11 ± 4	12 ± 4	285 ± 21	1380 ± 100
τ'(500 GeV)*	0.7 ± 0.1	7.4 ± 0.5	0.64 ± 0.13	3.71 ± 0.31
τ'(800 GeV)*	< 0.03	3.1 ± 0.2	< 0.03	0.06 ± 0.02
τ'(1000 GeV)*	< 0.03	1.2 ± 0.1	< 0.03	< 0.03

*Pre-fit

Table 9. Total observed yields as computed by the fit for control regions. The uncertainty contains both the systematic and statistical uncertainties. The prediction for each background sample is taken after a likelihood fit is performed to measure the VLL production cross section. Background normalization factors are also applied. The "Other Top" sample includes contributions from single top, $t\bar{t}$, $t\bar{t}+W$, $t+Z$, $t+WZ$, $t\bar{t}+H$, $t\bar{t}+WW$, $t\bar{t}t\bar{t}$, and ttt. The prediction from the signal samples is taken before the likelihood fit is performed. The background contributions may not add up to equal the total background due to rounding.

Uncertainty	$+\Delta\mu$	$-\Delta\mu$
Normalization factors	0.046	0.059
Fakes	0.033	0.050
Other theory uncertainties	0.017	0.012
τ-lepton ID and reconstruction	0.016	0.045
Light-lepton ID, reco., energy scale and momentum resolution	0.016	0.033
Jet energy scale and resolution, JVT, pileup reweighting	0.016	0.012
τ-lepton energy scale	0.011	0.010
$E_{\mathrm{T}}^{\mathrm{miss}}$	0.008	0.003
Luminosity	0.015	0.006
Flavour tagging	0.003	0.003
MC and fake-background statistical uncertainty	0.066	0.120
Total systematic uncertainty	0.098	0.160
Total statistical uncertainty	0.450	0.350

Table 10. Impact of each source of systematic uncertainty on the signal strength μ in the signal-plus-background fit. $M_{\tau'} = 900\,\mathrm{GeV}$ is considered. Both the positive and negative impacts on μ are considered. Individual sources of uncertainty are grouped for brevity but are treated as independent and uncorrelated in the fitting procedure. Impact of the total statistical uncertainty is also presented.

JHEP07(2023)118

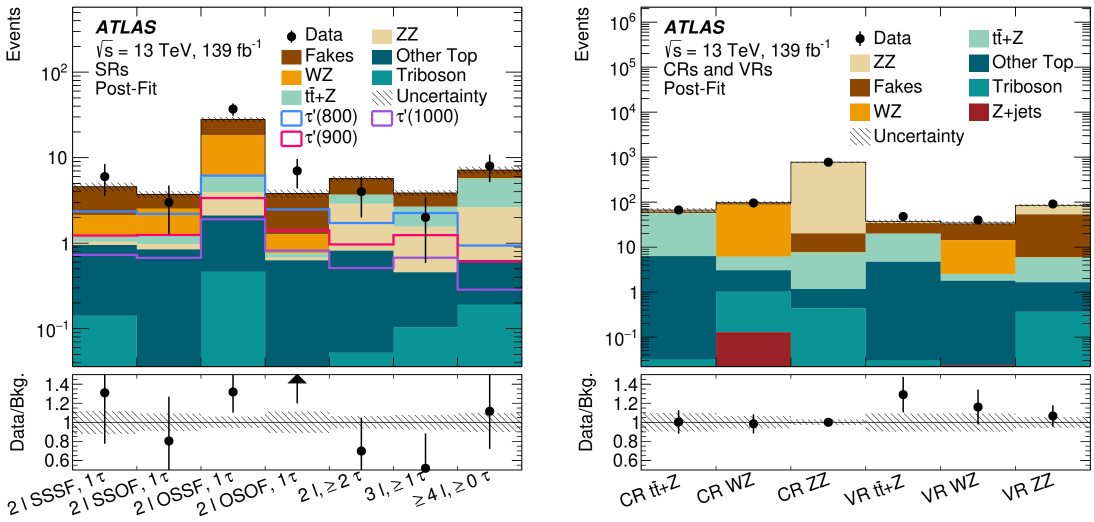

(a) (b)

Figure 4. Summary of post-fit yields for data and background, and pre-fit yields for signal modelling in the (a) SRs and (b) CRs and corresponding VRs. Uncertainty bands contain both the systematic and statistical uncertainties post-fit. Background normalization factors are also applied. The "Other Top" sample includes contributions from single top, $t\bar{t}$, $t\bar{t}+W$, $t+Z$, $t+WZ$, $t\bar{t}+H$, $t\bar{t}+WW$, $t\bar{t}t\bar{t}$, and ttt. The arrow in the ratio plot is for the point that is outside the range.

the expected significance decreases to ≈ 1 standard deviation at 1 TeV. The observed significance is found to be $\lessapprox 1$ standard deviation over the entire $M_{\tau'}$ range probed, as shown in table 11.

No significant deviation from the SM prediction is observed. Therefore, the 95% CL exclusion limit on the VLL production cross section as a function of $M_{\tau'}$ is calculated and shown in figure 6. In order to estimate the 95% CL upper limit on the VLL cross section, a simultaneous binned likelihood fit of the seven SRs and four CRs is performed, using the $\mathrm{CL_s}$ method [99] with the asymptotic approximation. The expected limit is shown with the black dashed line, and the shaded regions correspond to its one and two standard-deviation uncertainty bands. The observed 95% CL exclusion limit is shown with the solid black line. The expected lower limit on $M_{\tau'}$ is found to be 970 GeV, and the observed limit to be 900 GeV, by comparing the NLO theory prediction with the expected and observed 95% CL cross-section limits.

JHEP07(2023)118

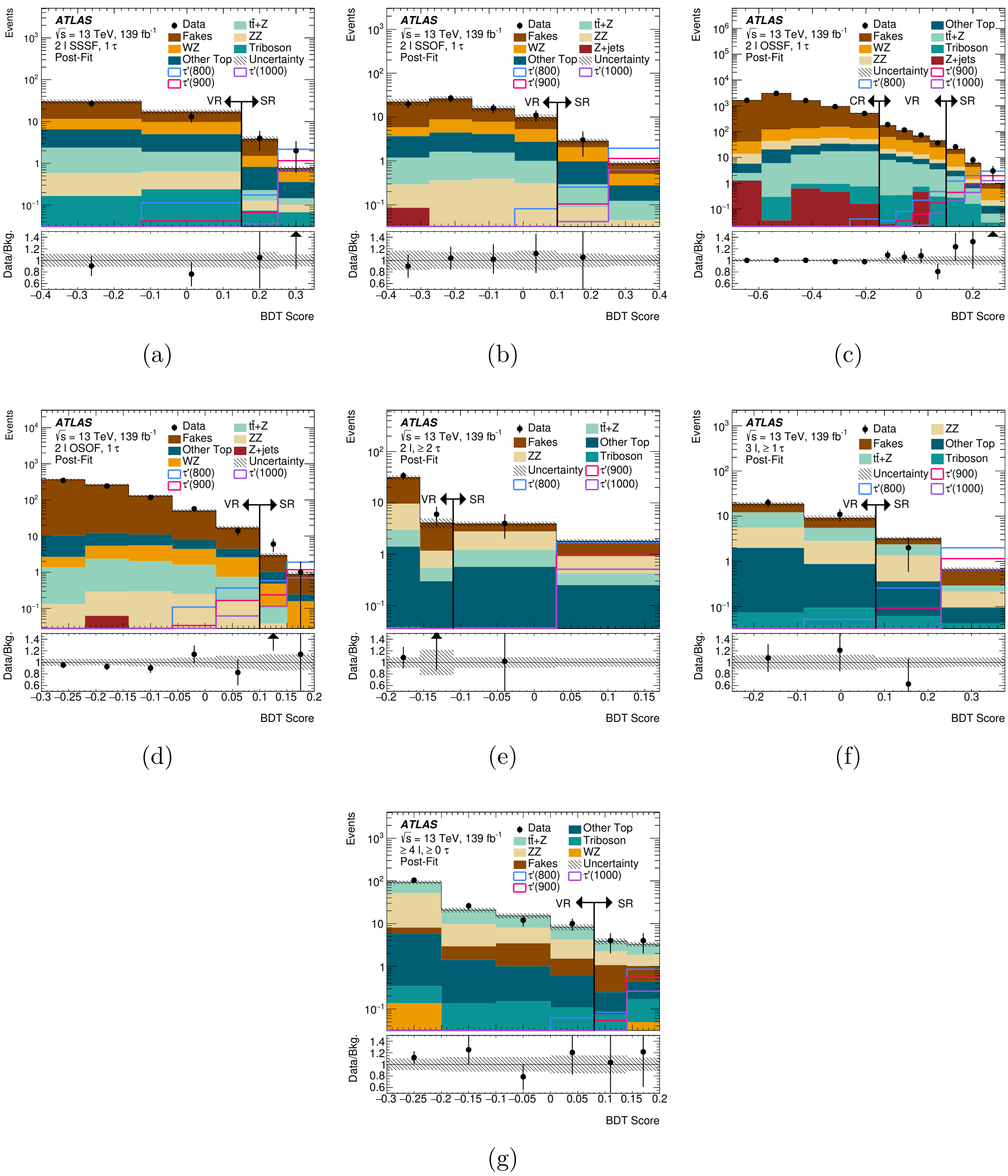

Figure 5. The post-fit BDT score distributions of data, background, and pre-fit signal modelling. The arrows indicate the point where there is a break between the regions and indicate the SRs used in the likelihood fit. The remaining distribution is treated as a VR and is not used in the fit (with the exception of (c) 2 ℓ OSSF, where the low BDT score region is used as a CR and is included in the fit); however, fitted nuisance parameters are propagated to these regions. The uncertainty bands contain both the systematic and statistical components post-fit. The first bin contains underflow events and the last bin contains overflow events. The arrows in the ratio plot are for points that are outside the range. (a) 2 ℓ SSSF, 1 τ; (b) 2 ℓ SSOF, 1 τ; (c) 2 ℓ OSSF, 1 τ; (d) 2 ℓ OSOF, 1 τ; (e) 2 ℓ, $\geq$ 2 τ; (f) 3 ℓ, $\geq$ 1 τ; (g) $\geq$ 4 ℓ, $\geq$ 0 τ.

JHEP07(2023)118

τ' Mass [GeV]	Significance		Exclusion Limit [fb]	
	Expected	Observed	Expected	Observed
130	5.9	−0.4	1110^{+520}_{-310}	953
200	12	−0.4	100^{+44}_{-28}	90
300	15	0.1	$17.0^{+7.5}_{-4.8}$	18
400	12	0.3	$7.4^{+3.3}_{-2.1}$	8.7
500	10	0.7	$3.6^{+1.6}_{-1.0}$	4.7
600	7.6	0.9	$2.3^{+1.0}_{-0.6}$	3.1
700	5.1	1.0	$1.8^{+0.8}_{-0.5}$	2.4
800	3.4	1.1	$1.5^{+0.7}_{-0.4}$	2.1
900	2.1	1.1	$1.3^{+0.6}_{-0.4}$	1.8
1000	1.3	1.2	$1.2^{+0.6}_{-0.3}$	1.7
1100	0.8	1.1	$1.2^{+0.6}_{-0.3}$	1.7
1200	0.5	1.1	$1.2^{+0.6}_{-0.3}$	1.7
1300	0.3	1.1	$1.2^{+0.6}_{-0.3}$	1.7

Table 11. Results from the fitting procedure for the VLL mass points studied. The expected and observed signal significances, and the 95% CL exclusion limits are shown.

JHEP07(2023)118

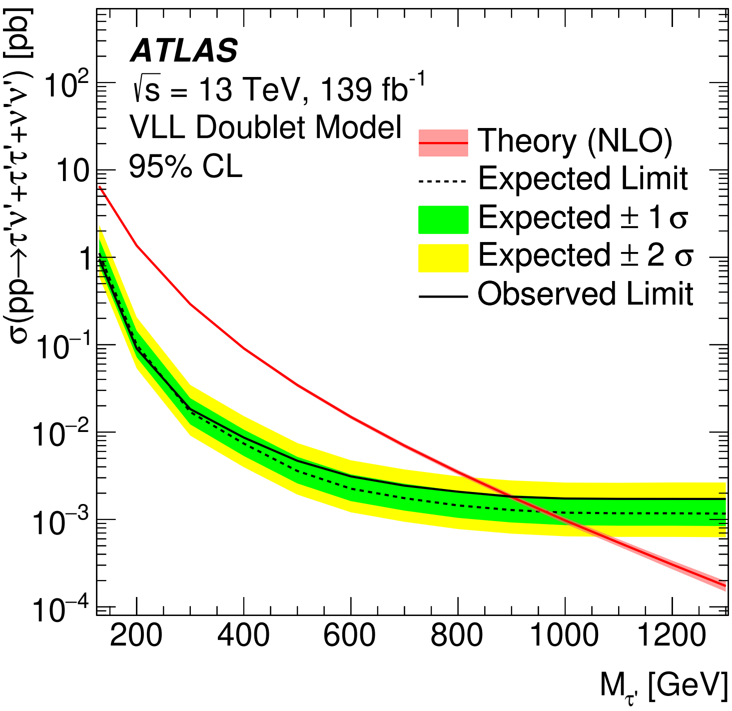

Figure 6. The 95% CL exclusion limit on the VLL production cross section as a function of VLL mass. The black dashed line represents the expected limit while the shaded regions are its one and two standard-deviation uncertainty bands. The solid black line is the observed limit as a function of VLL mass. The red curve is the NLO theory prediction along with its uncertainty.

JHEP07(2023)118

9 Conclusions

A search for vector-like leptons in a doublet model is performed using 139 fb^{-1} of pp collision data recorded at $\sqrt{s} = 13$ TeV by the ATLAS detector at the LHC. The search is performed using events with final states containing multiple light leptons and τ_{had}. Observing no excess of events above the SM expectation, a 95% CL upper limit on the cross section is calculated using the CL_s method. Using a doublet model where the vector-like leptons couple to the third-generation SM leptons, the observed mass range from 130 to 900 GeV is excluded at the 95% CL, while the highest excluded mass is expected to be 970 GeV.

Acknowledgments

We thank CERN for the very successful operation of the LHC, as well as the support staff from our institutions without whom ATLAS could not be operated efficiently.

We acknowledge the support of ANPCyT, Argentina; YerPhI, Armenia; ARC, Australia; BMWFW and FWF, Austria; ANAS, Azerbaijan; CNPq and FAPESP, Brazil; NSERC, NRC and CFI, Canada; CERN; ANID, Chile; CAS, MOST and NSFC, China; Minciencias, Colombia; MEYS CR, Czech Republic; DNRF and DNSRC, Denmark; IN2P3-CNRS and CEA-DRF/IRFU, France; SRNSFG, Georgia; BMBF, HGF and MPG, Germany; GSRI, Greece; RGC and Hong Kong SAR, China; ISF and Benoziyo Center, Israel; INFN, Italy; MEXT and JSPS, Japan; CNRST, Morocco; NWO, Netherlands; RCN, Norway; MEiN, Poland; FCT, Portugal; MNE/IFA, Romania; MESTD, Serbia; MSSR, Slovakia; ARRS and MIZŠ, Slovenia; DSI/NRF, South Africa; MICINN, Spain; SRC and Wallenberg Foundation, Sweden; SERI, SNSF and Cantons of Bern and Geneva, Switzerland; MOST, Taiwan; TENMAK, Türkiye; STFC, United Kingdom; DOE and NSF, United States of America. In addition, individual groups and members have received support from BCKDF, CANARIE, Compute Canada and CRC, Canada; PRIMUS 21/SCI/017 and UNCE SCI/013, Czech Republic; COST, ERC, ERDF, Horizon 2020 and Marie Skłodowska-Curie Actions, European Union; Investissements d'Avenir Labex, Investissements d'Avenir Idex and ANR, France; DFG and AvH Foundation, Germany; Herakleitos, Thales and Aristeia programmes co-financed by EU-ESF and the Greek NSRF, Greece; BSF-NSF and MINERVA, Israel; Norwegian Financial Mechanism 2014–2021, Norway; NCN and NAWA, Poland; La Caixa Banking Foundation, CERCA Programme Generalitat de Catalunya and PROMETEO and GenT Programmes Generalitat Valenciana, Spain; Göran Gustafssons Stiftelse, Sweden; The Royal Society and Leverhulme Trust, United Kingdom.

The crucial computing support from all WLCG partners is acknowledged gratefully, in particular from CERN, the ATLAS Tier-1 facilities at TRIUMF (Canada), NDGF (Denmark, Norway, Sweden), CC-IN2P3 (France), KIT/GridKA (Germany), INFN-CNAF (Italy), NL-T1 (Netherlands), PIC (Spain), ASGC (Taiwan), RAL (U.K.) and BNL (U.S.A.), the Tier-2 facilities worldwide and large non-WLCG resource providers. Major contributors of computing resources are listed in ref. [100].

References

[1] L. Evans and P. Bryant, *LHC Machine*, 2008 *JINST* **3** S08001 [INSPIRE].

[2] Particle Data Group collaboration, *Review of Particle Physics*, *PTEP* **2022** (2022) 083C01 [INSPIRE].

[3] S.P. Martin, *A supersymmetry primer*, *Adv. Ser. Direct. High Energy Phys.* **18** (1998) 1 [hep-ph/9709356] [INSPIRE].

[4] A. Djouadi and A. Lenz, *Sealing the fate of a fourth generation of fermions*, *Phys. Lett. B* **715** (2012) 310 [arXiv:1204.1252] [INSPIRE].

[5] O. Eberhardt et al., *Impact of a Higgs boson at a mass of 126 GeV on the standard model with three and four fermion generations*, *Phys. Rev. Lett.* **109** (2012) 241802 [arXiv:1209.1101] [INSPIRE].

[6] A. Lenz, *Constraints on a fourth generation of fermions from Higgs Boson searches*, *Adv. High Energy Phys.* **2013** (2013) 910275 [INSPIRE].

[7] P.H. Frampton, P.Q. Hung and M. Sher, *Quarks and leptons beyond the third generation*, *Phys. Rept.* **330** (2000) 263 [hep-ph/9903387] [INSPIRE].

[8] D0 collaboration, *Search for Single Vector-Like Quarks in $p\bar{p}$ Collisions at $\sqrt{s} = 1.96$ TeV*, *Phys. Rev. Lett.* **106** (2011) 081801 [arXiv:1010.1466] [INSPIRE].

[9] CDF collaboration, *Search for New Bottomlike Quark Pair Decays $Q\overline{Q} \to (tW^{\mp})(\bar{t}W^{\pm})$ in Same-Charge Dilepton Events*, *Phys. Rev. Lett.* **104** (2010) 091801 [arXiv:0912.1057] [INSPIRE].

[10] CMS collaboration, *Search for a Vectorlike Quark with Charge 2/3 in $t + Z$ Events from pp Collisions at $\sqrt{s} = 7$ TeV*, *Phys. Rev. Lett.* **107** (2011) 271802 [arXiv:1109.4985] [INSPIRE].

[11] CMS collaboration, *Search for pair produced fourth-generation up-type quarks in pp collisions at $\sqrt{s} = 7$ TeV with a lepton in the final state*, *Phys. Lett. B* **718** (2012) 307 [arXiv:1209.0471] [INSPIRE].

[12] ATLAS collaboration, *Search for Pair Production of a New b' Quark that Decays into a Z Boson and a Bottom Quark with the ATLAS Detector*, *Phys. Rev. Lett.* **109** (2012) 071801 [arXiv:1204.1265] [INSPIRE].

[13] CMS collaboration, *Search for vectorlike charge 2/3 T quarks in proton-proton collisions at $\sqrt{(s)} = 8$ TeV*, *Phys. Rev. D* **93** (2016) 012003 [arXiv:1509.04177] [INSPIRE].

[14] CMS collaboration, *Search for pair-produced vectorlike B quarks in proton-proton collisions at $\sqrt{s} = 8$ TeV*, *Phys. Rev. D* **93** (2016) 112009 [arXiv:1507.07129] [INSPIRE].

[15] CMS collaboration, *Inclusive search for a vector-like T quark with charge $\frac{2}{3}$ in pp collisions at $\sqrt{s} = 8$ TeV*, *Phys. Lett. B* **729** (2014) 149 [arXiv:1311.7667] [INSPIRE].

[16] CMS collaboration, *Search for vector-like T quarks decaying to top quarks and Higgs bosons in the all-hadronic channel using jet substructure*, *JHEP* **06** (2015) 080 [arXiv:1503.01952] [INSPIRE].

[17] ATLAS collaboration, *Search for pair production of a new heavy quark that decays into a W boson and a light quark in pp collisions at* $\sqrt{s} = 8$ *TeV with the ATLAS detector*, Phys. Rev. D **92** (2015) 112007 [arXiv:1509.04261] [INSPIRE].

[18] ATLAS collaboration, *Search for production of vector-like quark pairs and of four top quarks in the lepton-plus-jets final state in pp collisions at* $\sqrt{s} = 8$ *TeV with the ATLAS detector*, JHEP **08** (2015) 105 [arXiv:1505.04306] [INSPIRE].

[19] ATLAS collaboration, *Search for pair production of vector-like top quarks in events with one lepton, jets, and missing transverse momentum in* $\sqrt{s} = 13$ *TeV pp collisions with the ATLAS detector*, JHEP **08** (2017) 052 [arXiv:1705.10751] [INSPIRE].

[20] CMS collaboration, *Search for pair production of vector-like T and B quarks in single-lepton final states using boosted jet substructure techniques at* $\sqrt{s} = 13$ *TeV*, JHEP **11** (2017) 085 [arXiv:1706.03408] [INSPIRE].

[21] CMS collaboration, *Search for pair production of vector-like quarks in the* $bW\bar{b}W$ *channel from proton-proton collisions at* $\sqrt{s} = 13$ *TeV*, Phys. Lett. B **779** (2018) 82 [arXiv:1710.01539] [INSPIRE].

[22] CMS collaboration, *Search for vector-like T and B quark pairs in final states with leptons at* $\sqrt{s} = 13$ *TeV*, JHEP **08** (2018) 177 [arXiv:1805.04758] [INSPIRE].

[23] CMS collaboration, *Search for vector-like quarks in events with two oppositely charged leptons and jets in proton-proton collisions at* $\sqrt{s} = 13$ *TeV*, Eur. Phys. J. C **79** (2019) 364 [arXiv:1812.09768] [INSPIRE].

[24] ATLAS collaboration, *Search for pair production of heavy vector-like quarks decaying to high-*p_T *W bosons and b quarks in the lepton-plus-jets final state in pp collisions at* $\sqrt{s} = 13$ *TeV with the ATLAS detector*, JHEP **10** (2017) 141 [arXiv:1707.03347] [INSPIRE].

[25] ATLAS collaboration, *Search for pair production of up-type vector-like quarks and for four-top-quark events in final states with multiple b-jets with the ATLAS detector*, JHEP **07** (2018) 089 [arXiv:1803.09678] [INSPIRE].

[26] ATLAS collaboration, *Search for pair production of heavy vector-like quarks decaying into high-*p_T *W bosons and top quarks in the lepton-plus-jets final state in pp collisions at* $\sqrt{s} = 13$ *TeV with the ATLAS detector*, JHEP **08** (2018) 048 [arXiv:1806.01762] [INSPIRE].

[27] CMS collaboration, *Search for pair production of vector-like quarks in the fully hadronic final state*, Phys. Rev. D **100** (2019) 072001 [arXiv:1906.11903] [INSPIRE].

[28] CMS collaboration, *Search for pair-produced vector-like leptons in final states with third-generation leptons and at least three b quark jets in proton-proton collisions at* $\sqrt{s} = 13$ *TeV*, arXiv:2208.09700 [INSPIRE].

[29] L. Di Luzio, A. Greljo and M. Nardecchia, *Gauge leptoquark as the origin of B-physics anomalies*, Phys. Rev. D **96** (2017) 115011 [arXiv:1708.08450] [INSPIRE].

[30] L. Di Luzio et al., *Maximal flavour violation: a Cabibbo mechanism for leptoquarks*, JHEP **11** (2018) 081 [arXiv:1808.00942] [INSPIRE].

[31] A. Greljo and B.A. Stefanek, *Third family quark-lepton unification at the TeV scale*, Phys. Lett. B **782** (2018) 131 [arXiv:1802.04274] [INSPIRE].

[32] N. Kumar and S.P. Martin, *Vectorlike Leptons at the Large Hadron Collider*, Phys. Rev. D **92** (2015) 115018 [arXiv:1510.03456] [INSPIRE].

[33] P.N. Bhattiprolu and S.P. Martin, *Prospects for vectorlike leptons at future proton-proton colliders*, Phys. Rev. D **100** (2019) 015033 [arXiv:1905.00498] [INSPIRE].

[34] CMS collaboration, *Inclusive nonresonant multilepton probes of new phenomena at* $\sqrt{s} = 13$ *TeV*, Phys. Rev. D **105** (2022) 112007 [arXiv:2202.08676] [INSPIRE].

[35] J.M. Cornwall, D.N. Levin and G. Tiktopoulos, *Derivation of Gauge Invariance from High-Energy Unitarity Bounds on the S Matrix*, Phys. Rev. D **10** (1974) 1145 [*Erratum ibid.* **11** (1975) 972] [INSPIRE].

[36] Y. Freund and R.E. Schapire, *A decision-theoretic generalization of on-line learning and an application to boosting*, J. Comput. Syst. Sci. **55** (1997) 119 [INSPIRE].

[37] L. Breiman, J.H. Friedman, R.A. Olshen and C.J. Stone, *Classification and regression trees*, Routledge (2017) [DOI:10.1201/9781315139470].

[38] ATLAS collaboration, *The ATLAS Experiment at the CERN Large Hadron Collider*, 2008 *JINST* **3** S08003 [INSPIRE].

[39] ATLAS collaboration, *ATLAS Insertable B-Layer: Technical Design Report*, ATLAS-TDR-19 (2010).

[40] ATLAS IBL collaboration, *Production and integration of the ATLAS Insertable B-Layer*, 2018 *JINST* **13** T05008 [arXiv:1803.00844] [INSPIRE].

[41] ATLAS collaboration, *Performance of the ATLAS trigger system in 2015*, Eur. Phys. J. C **77** (2017) 317 [arXiv:1611.09661] [INSPIRE].

[42] ATLAS collaboration, *The ATLAS Collaboration Software and Firmware*, ATL-SOFT-PUB-2021-001, CERN, Geneva (2021).

[43] ATLAS collaboration, *ATLAS data quality operations and performance for 2015–2018 data-taking*, 2020 *JINST* **15** P04003 [arXiv:1911.04632] [INSPIRE].

[44] G. Avoni et al., *The new LUCID-2 detector for luminosity measurement and monitoring in ATLAS*, 2018 *JINST* **13** P07017 [INSPIRE].

[45] ATLAS collaboration, *Performance of electron and photon triggers in ATLAS during LHC Run 2*, Eur. Phys. J. C **80** (2020) 47 [arXiv:1909.00761] [INSPIRE].

[46] ATLAS collaboration, *Performance of the ATLAS muon triggers in Run 2*, 2020 *JINST* **15** P09015 [arXiv:2004.13447] [INSPIRE].

[47] GEANT4 collaboration, *GEANT4 — a simulation toolkit*, Nucl. Instrum. Meth. A **506** (2003) 250 [INSPIRE].

[48] ATLAS collaboration, *The ATLAS Simulation Infrastructure*, Eur. Phys. J. C **70** (2010) 823 [arXiv:1005.4568] [INSPIRE].

[49] T. Sjöstrand, S. Mrenna and P.Z. Skands, *A brief introduction to PYTHIA 8.1*, Comput. Phys. Commun. **178** (2008) 852 [arXiv:0710.3820] [INSPIRE].

[50] ATLAS collaboration, *The Pythia 8 A3 tune description of ATLAS minimum bias and inelastic measurements incorporating the Donnachie-Landshoff diffractive model*, ATL-PHYS-PUB-2016-017, CERN, Geneva (2016).

[51] R.D. Ball et al., *Parton distributions with LHC data*, Nucl. Phys. B **867** (2013) 244 [arXiv:1207.1303] [INSPIRE].

JHEP07(2023)118

[52] J. Alwall et al., *The automated computation of tree-level and next-to-leading order differential cross sections, and their matching to parton shower simulations*, *JHEP* **07** (2014) 079 [arXiv:1405.0301] [INSPIRE].

[53] SHERPA collaboration, *Event generation with Sherpa 2.2*, *SciPost Phys.* **7** (2019) 034 [arXiv:1905.09127] [INSPIRE].

[54] NNPDF collaboration, *Parton distributions for the LHC run II*, *JHEP* **04** (2015) 040 [arXiv:1410.8849] [INSPIRE].

[55] S. Schumann and F. Krauss, *A parton shower algorithm based on Catani-Seymour dipole factorisation*, *JHEP* **03** (2008) 038 [arXiv:0709.1027] [INSPIRE].

[56] S. Hoeche, F. Krauss, M. Schönherr and F. Siegert, *A critical appraisal of NLO+PS matching methods*, *JHEP* **09** (2012) 049 [arXiv:1111.1220] [INSPIRE].

[57] S. Hoeche, F. Krauss, M. Schönherr and F. Siegert, *QCD matrix elements + parton showers. The NLO case*, *JHEP* **04** (2013) 027 [arXiv:1207.5030] [INSPIRE].

[58] S. Catani, F. Krauss, R. Kuhn and B.R. Webber, *QCD Matrix Elements + Parton Showers*, *JHEP* **11** (2001) 063 [hep-ph/0109231] [INSPIRE].

[59] S. Hoeche, F. Krauss, S. Schumann and F. Siegert, *QCD matrix elements and truncated showers*, *JHEP* **05** (2009) 053 [arXiv:0903.1219] [INSPIRE].

[60] J.-C. Winter, F. Krauss and G. Soff, *A modified cluster-hadronization model*, *Eur. Phys. J. C* **36** (2004) 381 [hep-ph/0311085] [INSPIRE].

[61] T. Gleisberg and S. Hoeche, *Comix, a new matrix element generator*, *JHEP* **12** (2008) 039 [arXiv:0808.3674] [INSPIRE].

[62] OPENLOOPS 2 collaboration, *OpenLoops 2*, *Eur. Phys. J. C* **79** (2019) 866 [arXiv:1907.13071] [INSPIRE].

[63] F. Cascioli, P. Maierhöfer and S. Pozzorini, *Scattering Amplitudes with Open Loops*, *Phys. Rev. Lett.* **108** (2012) 111601 [arXiv:1111.5206] [INSPIRE].

[64] A. Denner, S. Dittmaier and L. Hofer, *COLLIER: A fortran-based complex one-loop library in extended regularizations*, *Comput. Phys. Commun.* **212** (2017) 220 [arXiv:1604.06792] [INSPIRE].

[65] S. Alioli, P. Nason, C. Oleari and E. Re, *A general framework for implementing NLO calculations in shower Monte Carlo programs: the POWHEG BOX*, *JHEP* **06** (2010) 043 [arXiv:1002.2581] [INSPIRE].

[66] P. Nason, *A new method for combining NLO QCD with shower Monte Carlo algorithms*, *JHEP* **11** (2004) 040 [hep-ph/0409146] [INSPIRE].

[67] S. Frixione, P. Nason and C. Oleari, *Matching NLO QCD computations with parton shower simulations: the POWHEG method*, *JHEP* **11** (2007) 070 [arXiv:0709.2092] [INSPIRE].

[68] ATLAS collaboration, *Studies on top-quark Monte Carlo modelling for Top2016*, ATL-PHYS-PUB-2016-020, CERN, Geneva (2016).

[69] S. Frixione et al., *Single-top hadroproduction in association with a W boson*, *JHEP* **07** (2008) 029 [arXiv:0805.3067] [INSPIRE].

[70] T. Sjöstrand et al., *An introduction to PYTHIA 8.2*, *Comput. Phys. Commun.* **191** (2015) 159 [arXiv:1410.3012] [INSPIRE].

[71] ATLAS collaboration, *Vertex Reconstruction Performance of the ATLAS Detector at* $\sqrt{s} = 13$ *TeV*, ATL-PHYS-PUB-2015-026, CERN, Geneva (2015).

[72] ATLAS collaboration, *Electron and photon performance measurements with the ATLAS detector using the 2015–2017 LHC proton-proton collision data*, 2019 *JINST* **14** P12006 [arXiv:1908.00005] [INSPIRE].

[73] ATLAS collaboration, *Muon reconstruction and identification efficiency in ATLAS using the full Run 2 pp collision data set at* $\sqrt{s} = 13$ *TeV*, *Eur. Phys. J. C* **81** (2021) 578 [arXiv:2012.00578] [INSPIRE].

[74] M. Cacciari, G.P. Salam and G. Soyez, *The anti-k_t jet clustering algorithm*, *JHEP* **04** (2008) 063 [arXiv:0802.1189] [INSPIRE].

[75] M. Cacciari and G.P. Salam, *Dispelling the N^3 myth for the k_t jet-finder*, *Phys. Lett. B* **641** (2006) 57 [hep-ph/0512210] [INSPIRE].

[76] M. Cacciari, G.P. Salam and G. Soyez, *FastJet user manual*, *Eur. Phys. J. C* **72** (2012) 1896 [arXiv:1111.6097] [INSPIRE].

[77] ATLAS collaboration, *Jet reconstruction and performance using particle flow with the ATLAS Detector*, *Eur. Phys. J. C* **77** (2017) 466 [arXiv:1703.10485] [INSPIRE].

[78] ATLAS collaboration, *Jet energy scale and resolution measured in proton-proton collisions at* $\sqrt{s} = 13$ *TeV with the ATLAS detector*, *Eur. Phys. J. C* **81** (2021) 689 [arXiv:2007.02645] [INSPIRE].

[79] ATLAS collaboration, *Performance of pile-up mitigation techniques for jets in pp collisions at* $\sqrt{s} = 8$ *TeV using the ATLAS detector*, *Eur. Phys. J. C* **76** (2016) 581 [arXiv:1510.03823] [INSPIRE].

[80] ATLAS collaboration, *ATLAS b-jet identification performance and efficiency measurement with $t\bar{t}$ events in pp collisions at* $\sqrt{s} = 13$ *TeV*, *Eur. Phys. J. C* **79** (2019) 970 [arXiv:1907.05120] [INSPIRE].

[81] ATLAS collaboration, *ATLAS flavour-tagging algorithms for the LHC Run 2 pp collision dataset*, arXiv:2211.16345 [INSPIRE].

[82] ATLAS collaboration, *Measurement of the tau lepton reconstruction and identification performance in the ATLAS experiment using pp collisions at* $\sqrt{s} = 13$ *TeV*, ATLAS-CONF-2017-029, CERN, Geneva (2017).

[83] ATLAS collaboration, *Reconstruction, Energy Calibration, and Identification of Hadronically Decaying Tau Leptons in the ATLAS Experiment for Run-2 of the LHC*, ATL-PHYS-PUB-2015-045, CERN, Geneva (2015).

[84] ATLAS collaboration, *Identification of hadronic tau lepton decays using neural networks in the ATLAS experiment*, ATL-PHYS-PUB-2019-033, CERN, Geneva (2019).

[85] ATLAS collaboration, *E_T^{miss} performance in the ATLAS detector using 2015–2016 LHC pp collisions*, ATLAS-CONF-2018-023, CERN, Geneva (2018).

[86] F. Pedregosa et al., *Scikit-learn: Machine learning in python*, *J. Machine Learning Res.* **12** (2011) 2825 [arXiv:1201.0490] [INSPIRE].

[87] ATLAS collaboration, *Search for doubly and singly charged Higgs bosons decaying into vector bosons in multi-lepton final states with the ATLAS detector using proton-proton collisions at* $\sqrt{s} = 13$ *TeV*, *JHEP* **06** (2021) 146 [arXiv:2101.11961] [INSPIRE].

JHEP07(2023)118

[88] ATLAS collaboration, *Tools for estimating fake/non-prompt lepton backgrounds with the ATLAS detector at the LHC*, arXiv:2211.16178 [INSPIRE].

[89] ATLAS collaboration, *Search for new phenomena in three- or four-lepton events in pp collisions at $\sqrt{s} = 13$ TeV with the ATLAS detector*, Phys. Lett. B **824** (2022) 136832 [arXiv:2107.00404] [INSPIRE].

[90] E. Bothmann, M. Schönherr and S. Schumann, *Reweighting QCD matrix-element and parton-shower calculations*, Eur. Phys. J. C **76** (2016) 590 [arXiv:1606.08753] [INSPIRE].

[91] J. Butterworth et al., *PDF4LHC recommendations for LHC Run II*, J. Phys. G **43** (2016) 023001 [arXiv:1510.03865] [INSPIRE].

[92] ATLAS collaboration, *Tagging and suppression of pileup jets with the ATLAS detector*, ATLAS-CONF-2014-018, CERN, Geneva (2014).

[93] ATLAS collaboration, *Muon reconstruction performance of the ATLAS detector in proton-proton collision data at $\sqrt{s} = 13$ TeV*, Eur. Phys. J. C **76** (2016) 292 [arXiv:1603.05598] [INSPIRE].

[94] ATLAS collaboration, *Jet energy scale measurements and their systematic uncertainties in proton-proton collisions at $\sqrt{s} = 13$ TeV with the ATLAS detector*, Phys. Rev. D **96** (2017) 072002 [arXiv:1703.09665] [INSPIRE].

[95] ATLAS collaboration, *Performance of missing transverse momentum reconstruction with the ATLAS detector using proton-proton collisions at $\sqrt{s} = 13$ TeV*, Eur. Phys. J. C **78** (2018) 903 [arXiv:1802.08168] [INSPIRE].

[96] W. Verkerke and D.P. Kirkby, *The RooFit toolkit for data modeling*, *eConf* **C0303241** (2003) MOLT007 [physics/0306116] [INSPIRE].

[97] L. Moneta et al., *The RooStats Project*, PoS **ACAT2010** (2010) 057 [arXiv:1009.1003] [INSPIRE].

[98] G. Cowan, K. Cranmer, E. Gross and O. Vitells, *Asymptotic formulae for likelihood-based tests of new physics*, Eur. Phys. J. C **71** (2011) 1554 [*Erratum ibid.* **73** (2013) 2501] [arXiv:1007.1727] [INSPIRE].

[99] A.L. Read, *Presentation of search results: the CL_S technique*, J. Phys. G **28** (2002) 2693 [INSPIRE].

[100] ATLAS collaboration, *ATLAS Computing Acknowledgements*, ATL-SOFT-PUB-2021-003, CERN, Geneva (2021).

The ATLAS collaboration

G. Aad[101], B. Abbott[119], D.C. Abbott[102], K. Abeling[55], S.H. Abidi[29], A. Aboulhorma[35e], H. Abramowicz[150], H. Abreu[149], Y. Abulaiti[116], A.C. Abusleme Hoffman[136a], B.S. Acharya[68a,68b,p], B. Achkar[55], C. Adam Bourdarios[4], L. Adamczyk[84a], L. Adamek[154], S.V. Addepalli[26], J. Adelman[114], A. Adiguzel[21c], S. Adorni[56], T. Adye[133], A.A. Affolder[135], Y. Afik[36], M.N. Agaras[13], J. Agarwala[72a,72b], A. Aggarwal[99], C. Agheorghiesei[27c], J.A. Aguilar-Saavedra[129f], A. Ahmad[36], F. Ahmadov[38,z], W.S. Ahmed[103], S. Ahuja[94], X. Ai[48], G. Aielli[75a,75b], I. Aizenberg[168], M. Akbiyik[99], T.P.A. Åkesson[97], A.V. Akimov[37], K. Al Khoury[41], G.L. Alberghi[23b], J. Albert[164], P. Albicocco[53], S. Alderweireldt[52], M. Aleksa[36], I.N. Aleksandrov[38], C. Alexa[27b], T. Alexopoulos[10], A. Alfonsi[113], F. Alfonsi[23b], M. Alhroob[119], B. Ali[131], S. Ali[147], M. Aliev[37], G. Alimonti[70a], W. Alkakhi[55], C. Allaire[66], B.M.M. Allbrooke[145], P.P. Allport[20], A. Aloisio[71a,71b], F. Alonso[89], C. Alpigiani[137], E. Alunno Camelia[75a,75b], M. Alvarez Estevez[98], M.G. Alviggi[71a,71b], M. Aly[100], Y. Amaral Coutinho[81b], A. Ambler[103], C. Amelung[36], M. Amerl[1], C.G. Ames[108], D. Amidei[105], S.P. Amor Dos Santos[129a], S. Amoroso[48], K.R. Amos[162], V. Ananiev[124], C. Anastopoulos[138], T. Andeen[11], J.K. Anders[36], S.Y. Andrean[47a,47b], A. Andreazza[70a,70b], S. Angelidakis[9], A. Angerami[41,ac], A.V. Anisenkov[37], A. Annovi[73a], C. Antel[56], M.T. Anthony[138], E. Antipov[120], M. Antonelli[53], D.J.A. Antrim[17a], F. Anulli[74a], M. Aoki[82], T. Aoki[152], J.A. Aparisi Pozo[162], M.A. Aparo[145], L. Aperio Bella[48], C. Appelt[18], N. Aranzabal[36], V. Araujo Ferraz[81a], C. Arcangeletti[53], A.T.H. Arce[51], E. Arena[91], J-F. Arguin[107], S. Argyropoulos[54], J.-H. Arling[48], A.J. Armbruster[36], O. Arnaez[154], H. Arnold[113], Z.P. Arrubarrena Tame[108], G. Artoni[74a,74b], H. Asada[110], K. Asai[117], S. Asai[152], N.A. Asbah[61], J. Assahsah[35d], K. Assamagan[29], R. Astalos[28a], R.J. Atkin[33a], M. Atkinson[161], N.B. Atlay[18], H. Atmani[62b], P.A. Atmasiddha[105], K. Augsten[131], S. Auricchio[71a,71b], A.D. Auriol[20], V.A. Austrup[170], G. Avner[149], G. Avolio[36], K. Axiotis[56], M.K. Ayoub[14c], G. Azuelos[107,ah], D. Babal[28a], H. Bachacou[134], K. Bachas[151,s], A. Bachiu[34], F. Backman[47a,47b], A. Badea[61], P. Bagnaia[74a,74b], M. Bahmani[18], A.J. Bailey[162], V.R. Bailey[161], J.T. Baines[133], C. Bakalis[10], O.K. Baker[171], P.J. Bakker[113], E. Bakos[15], D. Bakshi Gupta[8], S. Balaji[146], R. Balasubramanian[113], E.M. Baldin[37], P. Balek[132], E. Ballabene[70a,70b], F. Balli[134], L.M. Baltes[63a], W.K. Balunas[32], J. Balz[99], E. Banas[85], M. Bandieramonte[128], A. Bandyopadhyay[24], S. Bansal[24], L. Barak[150], E.L. Barberio[104], D. Barberis[57b,57a], M. Barbero[101], G. Barbour[95], K.N. Barends[33a], T. Barillari[109], M-S. Barisits[36], T. Barklow[142], R.M. Barnett[17a], P. Baron[121], D.A. Baron Moreno[100], A. Baroncelli[62a], G. Barone[29], A.J. Barr[125], L. Barranco Navarro[47a,47b], F. Barreiro[98], J. Barreiro Guimarães da Costa[14a], U. Barron[150], M.G. Barros Teixeira[129a], S. Barsov[37], F. Bartels[63a], R. Bartoldus[142], A.E. Barton[90], P. Bartos[28a], A. Basalaev[48], A. Basan[99], M. Baselga[49], I. Bashta[76a,76b], A. Bassalat[66,b], M.J. Basso[154], C.R. Basson[100], R.L. Bates[59], S. Batlamous[35e], J.R. Batley[32], B. Batool[140], M. Battaglia[135], D. Battulga[18], M. Bauce[74a,74b], P. Bauer[24], A. Bayirli[21a], J.B. Beacham[51], T. Beau[126], P.H. Beauchemin[157], F. Becherer[54], P. Bechtle[24],

JHEP07(2023)118

H.P. Beck[19,r], K. Becker[166], A.J. Beddall[21d], V.A. Bednyakov[38], C.P. Bee[144], L.J. Beemster[15], T.A. Beermann[36], M. Begalli[81d], M. Begel[29], A. Behera[144], J.K. Behr[48], C. Beirao Da Cruz E Silva[36], J.F. Beirer[55,36], F. Beisiegel[24], M. Belfkir[158], G. Bella[150], L. Bellagamba[23b], A. Bellerive[34], P. Bellos[20], K. Beloborodov[37], K. Belotskiy[37], N.L. Belyaev[37], D. Benchekroun[35a], F. Bendebba[35a], Y. Benhammou[150], D.P. Benjamin[29], M. Benoit[29], J.R. Bensinger[26], S. Bentvelsen[113], L. Beresford[36], M. Beretta[53], D. Berge[18], E. Bergeaas Kuutmann[160], N. Berger[4], B. Bergmann[131], J. Beringer[17a], S. Berlendis[7], G. Bernardi[5], C. Bernius[142], F.U. Bernlochner[24], T. Berry[94], P. Berta[132], A. Berthold[50], I.A. Bertram[90], S. Bethke[109], A. Betti[74a,74b], A.J. Bevan[93], M. Bhamjee[33c], S. Bhatta[144], D.S. Bhattacharya[165], P. Bhattarai[26], V.S. Bhopatkar[120], R. Bi[29,ak], R.M. Bianchi[128], O. Biebel[108], R. Bielski[122], M. Biglietti[76a], T.R.V. Billoud[131], M. Bindi[55], A. Bingul[21b], C. Bini[74a,74b], S. Biondi[23b,23a], A. Biondini[91], C.J. Birch-sykes[100], G.A. Bird[20,133], M. Birman[168], T. Bisanz[36], E. Bisceglie[43b,43a], D. Biswas[169,l], A. Bitadze[100], K. Bjørke[124], I. Bloch[48], C. Blocker[26], A. Blue[59], U. Blumenschein[93], J. Blumenthal[99], G.J. Bobbink[113], V.S. Bobrovnikov[37], M. Boehler[54], D. Bogavac[36], A.G. Bogdanchikov[37], C. Bohm[47a], V. Boisvert[94], P. Bokan[48], T. Bold[84a], M. Bomben[5], M. Bona[93], M. Boonekamp[134], C.D. Booth[94], A.G. Borbély[59], H.M. Borecka-Bielska[107], L.S. Borgna[95], G. Borissov[90], D. Bortoletto[125], D. Boscherini[23b], M. Bosman[13], J.D. Bossio Sola[36], K. Bouaouda[35a], N. Bouchhar[162], J. Boudreau[128], E.V. Bouhova-Thacker[90], D. Boumediene[40], R. Bouquet[5], A. Boveia[118], J. Boyd[36], D. Boye[29], I.R. Boyko[38], J. Bracinik[20], N. Brahimi[62d], G. Brandt[170], O. Brandt[32], F. Braren[48], B. Brau[102], J.E. Brau[122], K. Brendlinger[48], R. Brener[168], L. Brenner[113], R. Brenner[160], S. Bressler[168], B. Brickwedde[99], D. Britton[59], D. Britzger[109], I. Brock[24], G. Brooijmans[41], W.K. Brooks[136f], E. Brost[29], T.L. Bruckler[125], P.A. Bruckman de Renstrom[85], B. Brüers[48], D. Bruncko[28b,*], A. Bruni[23b], G. Bruni[23b], M. Bruschi[23b], N. Bruscino[74a,74b], L. Bryngemark[142], T. Buanes[16], Q. Buat[137], P. Buchholz[140], A.G. Buckley[59], I.A. Budagov[38,*], M.K. Bugge[124], O. Bulekov[37], B.A. Bullard[61], S. Burdin[91], C.D. Burgard[48], A.M. Burger[40], B. Burghgrave[8], J.T.P. Burr[32], C.D. Burton[11], J.C. Burzynski[141], E.L. Busch[41], V. Büscher[99], P.J. Bussey[59], J.M. Butler[25], C.M. Buttar[59], J.M. Butterworth[95], W. Buttinger[133], C.J. Buxo Vazquez[106], A.R. Buzykaev[37], G. Cabras[23b], S. Cabrera Urbán[162], D. Caforio[58], H. Cai[128], Y. Cai[14a,14d], V.M.M. Cairo[36], O. Cakir[3a], N. Calace[36], P. Calafiura[17a], G. Calderini[126], P. Calfayan[67], G. Callea[59], L.P. Caloba[81b], D. Calvet[40], S. Calvet[40], T.P. Calvet[101], M. Calvetti[73a,73b], R. Camacho Toro[126], S. Camarda[36], D. Camarero Munoz[26], P. Camarri[75a,75b], M.T. Camerlingo[76a,76b], D. Cameron[124], C. Camincher[164], M. Campanelli[95], A. Camplani[42], V. Canale[71a,71b], A. Canesse[103], M. Cano Bret[79], J. Cantero[162], Y. Cao[161], F. Capocasa[26], M. Capua[43b,43a], A. Carbone[70a,70b], R. Cardarelli[75a], J.C.J. Cardenas[8], F. Cardillo[162], T. Carli[36], G. Carlino[71a], J.I. Carlotto[13], B.T. Carlson[128,t], E.M. Carlson[164,155a], L. Carminati[70a,70b], M. Carnesale[74a,74b], S. Caron[112], E. Carquin[136f], S. Carrá[70a,70b], G. Carratta[23b,23a], F. Carrio Argos[33g], J.W.S. Carter[154], T.M. Carter[52], M.P. Casado[13,i], A.F. Casha[154], E.G. Castiglia[171], F.L. Castillo[63a], L. Castillo Garcia[13],

V. Castillo Gimenez[162], N.F. Castro[129a,129e], A. Catinaccio[36], J.R. Catmore[124], V. Cavaliere[29], N. Cavalli[23b,23a], V. Cavasinni[73a,73b], E. Celebi[21a], F. Celli[125], M.S. Centonze[69a,69b], K. Cerny[121], A.S. Cerqueira[81a], A. Cerri[145], L. Cerrito[75a,75b], F. Cerutti[17a], A. Cervelli[23b], S.A. Cetin[21d], Z. Chadi[35a], D. Chakraborty[114], M. Chala[129f], J. Chan[169], W.Y. Chan[152], J.D. Chapman[32], B. Chargeishvili[148b], D.G. Charlton[20], T.P. Charman[93], M. Chatterjee[19], S. Chekanov[6], S.V. Chekulaev[155a], G.A. Chelkov[38,a], A. Chen[105], B. Chen[150], B. Chen[164], H. Chen[14c], H. Chen[29], J. Chen[62c], J. Chen[26], S. Chen[152], S.J. Chen[14c], X. Chen[62c], X. Chen[14b,ag], Y. Chen[62a], C.L. Cheng[169], H.C. Cheng[64a], S. Cheong[142], A. Cheplakov[38], E. Cheremushkina[48], E. Cherepanova[113], R. Cherkaoui El Moursli[35e], E. Cheu[7], K. Cheung[65], L. Chevalier[134], V. Chiarella[53], G. Chiarelli[73a], N. Chiedde[101], G. Chiodini[69a], A.S. Chisholm[20], A. Chitan[27b], M. Chitishvili[162], Y.H. Chiu[164], M.V. Chizhov[38], K. Choi[11], A.R. Chomont[74a,74b], Y. Chou[102], E.Y.S. Chow[113], T. Chowdhury[33g], L.D. Christopher[33g], K.L. Chu[64a], M.C. Chu[64a], X. Chu[14a,14d], J. Chudoba[130], J.J. Chwastowski[85], D. Cieri[109], K.M. Ciesla[84a], V. Cindro[92], A. Ciocio[17a], F. Cirotto[71a,71b], Z.H. Citron[168,m], M. Citterio[70a], D.A. Ciubotaru[27b], B.M. Ciungu[154], A. Clark[56], P.J. Clark[52], J.M. Clavijo Columbie[48], S.E. Clawson[100], C. Clement[47a,47b], J. Clercx[48], L. Clissa[23b,23a], Y. Coadou[101], M. Cobal[68a,68c], A. Coccaro[57b], R.F. Coelho Barrue[129a], R. Coelho Lopes De Sa[102], S. Coelli[70a], H. Cohen[150], A.E.C. Coimbra[70a,70b], B. Cole[41], J. Collot[60], P. Conde Muiño[129a,129g], M.P. Connell[33c], S.H. Connell[33c], I.A. Connelly[59], E.I. Conroy[125], F. Conventi[71a,ai], H.G. Cooke[20], A.M. Cooper-Sarkar[125], F. Cormier[163], L.D. Corpe[36], M. Corradi[74a,74b], E.E. Corrigan[97], F. Corriveau[103,x], A. Cortes-Gonzalez[18], M.J. Costa[162], F. Costanza[4], D. Costanzo[138], B.M. Cote[118], G. Cowan[94], J.W. Cowley[32], K. Cranmer[116], S. Crépé-Renaudin[60], F. Crescioli[126], M. Cristinziani[140], M. Cristoforetti[77a,77b,d], V. Croft[157], G. Crosetti[43b,43a], A. Cueto[36], T. Cuhadar Donszelmann[159], H. Cui[14a,14d], Z. Cui[7], A.R. Cukierman[142], W.R. Cunningham[59], F. Curcio[43b,43a], P. Czodrowski[36], M.M. Czurylo[63b], M.J. Da Cunha Sargedas De Sousa[62a], J.V. Da Fonseca Pinto[81b], C. Da Via[100], W. Dabrowski[84a], T. Dado[49], S. Dahbi[33g], T. Dai[105], C. Dallapiccola[102], M. Dam[42], G. D'amen[29], V. D'Amico[108], J. Damp[99], J.R. Dandoy[127], M.F. Daneri[30], M. Danninger[141], V. Dao[36], G. Darbo[57b], S. Darmora[6], S.J. Das[29,ak], S. D'Auria[70a,70b], C. David[155b], T. Davidek[132], D.R. Davis[51], B. Davis-Purcell[34], I. Dawson[93], K. De[8], R. De Asmundis[71a], M. De Beurs[113], N. De Biase[48], S. De Castro[23b,23a], N. De Groot[112], P. de Jong[113], H. De la Torre[106], A. De Maria[14c], A. De Salvo[74a], U. De Sanctis[75a,75b], A. De Santo[145], J.B. De Vivie De Regie[60], D.V. Dedovich[38], J. Degens[113], A.M. Deiana[44], F. Del Corso[23b,23a], J. Del Peso[98], F. Del Rio[63a], F. Deliot[134], C.M. Delitzsch[49], M. Della Pietra[71a,71b], D. Della Volpe[56], A. Dell'Acqua[36], L. Dell'Asta[70a,70b], M. Delmastro[4], P.A. Delsart[60], S. Demers[171], M. Demichev[38], S.P. Denisov[37], L. D'Eramo[114], D. Derendarz[85], F. Derue[126], P. Dervan[91], K. Desch[24], K. Dette[154], C. Deutsch[24], P.O. Deviveiros[36], F.A. Di Bello[57b,57a], A. Di Ciaccio[75a,75b], L. Di Ciaccio[4], A. Di Domenico[74a,74b], C. Di Donato[71a,71b], A. Di Girolamo[36], G. Di Gregorio[5], A. Di Luca[77a,77b], B. Di Micco[76a,76b], R. Di Nardo[76a,76b], C. Diaconu[101], F.A. Dias[113], T. Dias Do Vale[141],

JHEP07(2023)118

M.A. Diaz[136a,136b], F.G. Diaz Capriles[24], M. Didenko[162], E.B. Diehl[105], L. Diehl[54], S. Díez Cornell[48], C. Diez Pardos[140], C. Dimitriadi[24,160], A. Dimitrievska[17a], W. Ding[14b], J. Dingfelder[24], I-M. Dinu[27b], S.J. Dittmeier[63b], F. Dittus[36], F. Djama[101], T. Djobava[148b], J.I. Djuvsland[16], C. Doglioni[100,97], J. Dolejsi[132], Z. Dolezal[132], M. Donadelli[81c], B. Dong[62c], J. Donini[40], A. D'Onofrio[14c], M. D'Onofrio[91], J. Dopke[133], A. Doria[71a], M.T. Dova[89], A.T. Doyle[59], M.A. Draguet[125], E. Drechsler[141], E. Dreyer[168], I. Drivas-koulouris[10], A.S. Drobac[157], M. Drozdova[56], D. Du[62a], T.A. du Pree[113], F. Dubinin[37], M. Dubovsky[28a], E. Duchovni[168], G. Duckeck[108], O.A. Ducu[27b], D. Duda[109], A. Dudarev[36], M. D'uffizi[100], L. Duflot[66], M. Dührssen[36], C. Dülsen[170], A.E. Dumitriu[27b], M. Dunford[63a], S. Dungs[49], K. Dunne[47a,47b], A. Duperrin[101], H. Duran Yildiz[3a], M. Düren[58], A. Durglishvili[148b], B.L. Dwyer[114], G.I. Dyckes[17a], M. Dyndal[84a], S. Dysch[100], B.S. Dziedzic[85], Z.O. Earnshaw[145], B. Eckerova[28a], M.G. Eggleston[51], E. Egidio Purcino De Souza[81b], L.F. Ehrke[56], G. Eigen[16], K. Einsweiler[17a], T. Ekelof[160], P.A. Ekman[97], Y. El Ghazali[35b], H. El Jarrari[35e,147], A. El Moussaouy[35a], V. Ellajosyula[160], M. Ellert[160], F. Ellinghaus[170], A.A. Elliot[93], N. Ellis[36], J. Elmsheuser[29], M. Elsing[36], D. Emeliyanov[133], A. Emerman[41], Y. Enari[152], I. Ene[17a], S. Epari[13], J. Erdmann[49,ae], A. Ereditato[19], P.A. Erland[85], M. Errenst[170], M. Escalier[66], C. Escobar[162], E. Etzion[150], G. Evans[129a], H. Evans[67], M.O. Evans[145], A. Ezhilov[37], S. Ezzarqtouni[35a], F. Fabbri[59], L. Fabbri[23b,23a], G. Facini[95], V. Fadeyev[135], R.M. Fakhrutdinov[37], S. Falciano[74a], P.J. Falke[24], S. Falke[36], J. Faltova[132], Y. Fan[14a], Y. Fang[14a,14d], G. Fanourakis[46], M. Fanti[70a,70b], M. Faraj[68a,68b], Z. Farazpay[96], A. Farbin[8], A. Farilla[76a], T. Farooque[106], S.M. Farrington[52], F. Fassi[35e], D. Fassouliotis[9], M. Faucci Giannelli[75a,75b], W.J. Fawcett[32], L. Fayard[66], P. Federicova[130], O.L. Fedin[37,a], G. Fedotov[37], M. Feickert[169], L. Feligioni[101], A. Fell[138], D.E. Fellers[122], C. Feng[62b], M. Feng[14b], Z. Feng[113], M.J. Fenton[159], A.B. Fenyuk[37], L. Ferencz[48], S.W. Ferguson[45], J. Ferrando[48], A. Ferrari[160], P. Ferrari[113,112], R. Ferrari[72a], D. Ferrere[56], C. Ferretti[105], F. Fiedler[99], A. Filipčič[92], E.K. Filmer[1], F. Filthaut[112], M.C.N. Fiolhais[129a,129c,c], L. Fiorini[162], F. Fischer[140], W.C. Fisher[106], T. Fitschen[100], I. Fleck[140], P. Fleischmann[105], T. Flick[170], L. Flores[127], M. Flores[33d,ad], L.R. Flores Castillo[64a], F.M. Follega[77a,77b], N. Fomin[16], J.H. Foo[154], B.C. Forland[67], A. Formica[134], A.C. Forti[100], E. Fortin[101], A.W. Fortman[61], M.G. Foti[17a], L. Fountas[9,j], D. Fournier[66], H. Fox[90], P. Francavilla[73a,73b], S. Francescato[61], S. Franchellucci[56], M. Franchini[23b,23a], S. Franchino[63a], D. Francis[36], L. Franco[112], L. Franconi[19], M. Franklin[61], G. Frattari[26], A.C. Freegard[93], P.M. Freeman[20], W.S. Freund[81b], N. Fritzsche[50], A. Froch[54], D. Froidevaux[36], J.A. Frost[125], Y. Fu[62a], M. Fujimoto[117], E. Fullana Torregrosa[162,*], J. Fuster[162], A. Gabrielli[23b,23a], A. Gabrielli[154], P. Gadow[48], G. Gagliardi[57b,57a], L.G. Gagnon[17a], G.E. Gallardo[125], E.J. Gallas[125], B.J. Gallop[133], R. Gamboa Goni[93], K.K. Gan[118], S. Ganguly[152], J. Gao[62a], Y. Gao[52], F.M. Garay Walls[136a,136b], B. Garcia[29,ak], C. García[162], J.E. García Navarro[162], J.A. García Pascual[14a], M. Garcia-Sciveres[17a], R.W. Gardner[39], D. Garg[79], R.B. Garg[142,q], S. Gargiulo[54], C.A. Garner[154], V. Garonne[29], S.J. Gasiorowski[137], P. Gaspar[81b], G. Gaudio[72a], V. Gautam[13],

JHEP07(2023)118

P. Gauzzi[74a,74b], I.L. Gavrilenko[37], A. Gavrilyuk[37], C. Gay[163], G. Gaycken[48], E.N. Gazis[10], A.A. Geanta[27b,27e], C.M. Gee[135], J. Geisen[97], M. Geisen[99], C. Gemme[57b], M.H. Genest[60], S. Gentile[74a,74b], S. George[94], W.F. George[20], T. Geralis[46], L.O. Gerlach[55], P. Gessinger-Befurt[36], M. Ghasemi Bostanabad[164], M. Ghneimat[140], K. Ghorbanian[93], A. Ghosal[140], A. Ghosh[159], A. Ghosh[7], B. Giacobbe[23b], S. Giagu[74a,74b], N. Giangiacomi[154], P. Giannetti[73a], A. Giannini[62a], S.M. Gibson[94], M. Gignac[135], D.T. Gil[84b], A.K. Gilbert[84a], B.J. Gilbert[41], D. Gillberg[34], G. Gilles[113], N.E.K. Gillwald[48], L. Ginabat[126], D.M. Gingrich[2,ah], M.P. Giordani[68a,68c], P.F. Giraud[134], G. Giugliarelli[68a,68c], D. Giugni[70a], F. Giuli[36], I. Gkialas[9,j], L.K. Gladilin[37], C. Glasman[98], G.R. Gledhill[122], M. Glisic[122], I. Gnesi[43b,f], Y. Go[29,ak], M. Goblirsch-Kolb[26], B. Gocke[49], D. Godin[107], S. Goldfarb[104], T. Golling[56], M.G.D. Gololo[33g], D. Golubkov[37], J.P. Gombas[106], A. Gomes[129a,129b], G. Gomes Da Silva[140], A.J. Gomez Delegido[162], R. Goncalves Gama[55], R. Gonçalo[129a,129c], G. Gonella[122], L. Gonella[20], A. Gongadze[38], F. Gonnella[20], J.L. Gonski[41], R.Y. González Andana[52], S. González de la Hoz[162], S. Gonzalez Fernandez[13], R. Gonzalez Lopez[91], C. Gonzalez Renteria[17a], R. Gonzalez Suarez[160], S. Gonzalez-Sevilla[56], G.R. Gonzalvo Rodriguez[162], L. Goossens[36], N.A. Gorasia[20], P.A. Gorbounov[37], B. Gorini[36], E. Gorini[69a,69b], A. Gorišek[92], A.T. Goshaw[51], M.I. Gostkin[38], C.A. Gottardo[36], M. Gouighri[35b], V. Goumarre[48], A.G. Goussiou[137], N. Govender[33c], C. Goy[4], I. Grabowska-Bold[84a], K. Graham[34], E. Gramstad[124], S. Grancagnolo[18], M. Grandi[145], V. Gratchev[37,*], P.M. Gravila[27f], F.G. Gravili[69a,69b], H.M. Gray[17a], M. Greco[69a,69b], C. Grefe[24], I.M. Gregor[48], P. Grenier[142], C. Grieco[13], A.A. Grillo[135], K. Grimm[31,n], S. Grinstein[13,v], J.-F. Grivaz[66], E. Gross[168], J. Grosse-Knetter[55], C. Grud[105], A. Grummer[111], J.C. Grundy[125], L. Guan[105], W. Guan[169], C. Gubbels[163], J.G.R. Guerrero Rojas[162], G. Guerrieri[68a,68b], F. Guescini[109], R. Gugel[99], J.A.M. Guhit[105], A. Guida[48], T. Guillemin[4], E. Guilloton[166,133], S. Guindon[36], F. Guo[14a,14d], J. Guo[62c], L. Guo[66], Y. Guo[105], R. Gupta[48], S. Gurbuz[24], S.S. Gurdasani[54], G. Gustavino[36], M. Guth[56], P. Gutierrez[119], L.F. Gutierrez Zagazeta[127], C. Gutschow[95], C. Guyot[134], C. Gwenlan[125], C.B. Gwilliam[91], E.S. Haaland[124], A. Haas[116], M. Habedank[48], C. Haber[17a], H.K. Hadavand[8], A. Hadef[99], S. Hadzic[109], E.H. Haines[95], M. Haleem[165], J. Haley[120], J.J. Hall[138], G.D. Hallewell[101], L. Halser[19], K. Hamano[164], H. Hamdaoui[35e], M. Hamer[24], G.N. Hamity[52], J. Han[62b], K. Han[62a], L. Han[14c], L. Han[62a], S. Han[17a], Y.F. Han[154], K. Hanagaki[82], M. Hance[135], D.A. Hangal[41,ac], H. Hanif[141], M.D. Hank[39], R. Hankache[100], J.B. Hansen[42], J.D. Hansen[42], P.H. Hansen[42], K. Hara[156], D. Harada[56], T. Harenberg[170], S. Harkusha[37], Y.T. Harris[125], N.M. Harrison[118], P.F. Harrison[166], N.M. Hartman[142], N.M. Hartmann[108], Y. Hasegawa[139], A. Hasib[52], S. Haug[19], R. Hauser[106], M. Havranek[131], C.M. Hawkes[20], R.J. Hawkings[36], S. Hayashida[110], D. Hayden[106], C. Hayes[105], R.L. Hayes[163], C.P. Hays[125], J.M. Hays[93], H.S. Hayward[91], F. He[62a], Y. He[153], Y. He[126], M.P. Heath[52], V. Hedberg[97], A.L. Heggelund[124], N.D. Hehir[93], C. Heidegger[54], K.K. Heidegger[54], W.D. Heidorn[80], J. Heilman[34], S. Heim[48], T. Heim[17a], J.G. Heinlein[127], J.J. Heinrich[122], L. Heinrich[109,af], J. Hejbal[130],

L. Helary[48], A. Held[169], S. Hellesund[124], C.M. Helling[163], S. Hellman[47a,47b], C. Helsens[36], R.C.W. Henderson[90], L. Henkelmann[32], A.M. Henriques Correia[36], H. Herde[97], Y. Hernández Jiménez[144], L.M. Herrmann[24], M.G. Herrmann[108], T. Herrmann[50], G. Herten[54], R. Hertenberger[108], L. Hervas[36], N.P. Hessey[155a], H. Hibi[83], E. Higón-Rodriguez[162], S.J. Hillier[20], I. Hinchliffe[17a], F. Hinterkeuser[24], M. Hirose[123], S. Hirose[156], D. Hirschbuehl[170], T.G. Hitchings[100], B. Hiti[92], J. Hobbs[144], R. Hobincu[27e], N. Hod[168], M.C. Hodgkinson[138], B.H. Hodkinson[32], A. Hoecker[36], J. Hofer[48], D. Hohn[54], T. Holm[24], M. Holzbock[109], L.B.A.H. Hommels[32], B.P. Honan[100], J. Hong[62c], T.M. Hong[128], J.C. Honig[54], A. Hönle[109], B.H. Hooberman[161], W.H. Hopkins[6], Y. Horii[110], S. Hou[147], A.S. Howard[92], J. Howarth[59], J. Hoya[6], M. Hrabovsky[121], A. Hrynevich[48], T. Hryn'ova[4], P.J. Hsu[65], S.-C. Hsu[137], Q. Hu[41,ac], Y.F. Hu[14a,14d,aj], D.P. Huang[95], S. Huang[64b], X. Huang[14c], Y. Huang[62a], Y. Huang[14a], Z. Huang[100], Z. Hubacek[131], M. Huebner[24], F. Huegging[24], T.B. Huffman[125], M. Huhtinen[36], S.K. Huiberts[16], R. Hulsken[103], N. Huseynov[12,a], J. Huston[106], J. Huth[61], R. Hyneman[142], S. Hyrych[28a], G. Iacobucci[56], G. Iakovidis[29], I. Ibragimov[140], L. Iconomidou-Fayard[66], P. Iengo[71a,71b], R. Iguchi[152], T. Iizawa[56], Y. Ikegami[82], A. Ilg[19], N. Ilic[154], H. Imam[35a], T. Ingebretsen Carlson[47a,47b], G. Introzzi[72a,72b], M. Iodice[76a], V. Ippolito[74a,74b], M. Ishino[152], W. Islam[169], C. Issever[18,48], S. Istin[21a,am], H. Ito[167], J.M. Iturbe Ponce[64a], R. Iuppa[77a,77b], A. Ivina[168], J.M. Izen[45], V. Izzo[71a], P. Jacka[130,131], P. Jackson[1], R.M. Jacobs[48], B.P. Jaeger[141], C.S. Jagfeld[108], G. Jäkel[170], K. Jakobs[54], T. Jakoubek[168], J. Jamieson[59], K.W. Janas[84a], G. Jarlskog[97], A.E. Jaspan[91], M. Javurkova[102], F. Jeanneau[134], L. Jeanty[122], J. Jejelava[148a,aa], P. Jenni[54,g], C.E. Jessiman[34], S. Jézéquel[4], J. Jia[144], X. Jia[61], X. Jia[14a,14d], Z. Jia[14c], Y. Jiang[62a], S. Jiggins[52], J. Jimenez Pena[109], S. Jin[14c], A. Jinaru[27b], O. Jinnouchi[153], P. Johansson[138], K.A. Johns[7], D.M. Jones[32], E. Jones[166], P. Jones[32], R.W.L. Jones[90], T.J. Jones[91], R. Joshi[118], J. Jovicevic[15], X. Ju[17a], J.J. Junggeburth[36], A. Juste Rozas[13,v], S. Kabana[136e], A. Kaczmarska[85], M. Kado[74a,74b], H. Kagan[118], M. Kagan[142], A. Kahn[41], A. Kahn[127], C. Kahra[99], T. Kaji[167], E. Kajomovitz[149], N. Kakati[168], C.W. Kalderon[29], A. Kamenshchikov[154], S. Kanayama[153], N.J. Kang[135], Y. Kano[110], D. Kar[33g], K. Karava[125], M.J. Kareem[155b], E. Karentzos[54], I. Karkanias[151], S.N. Karpov[38], Z.M. Karpova[38], V. Kartvelishvili[90], A.N. Karyukhin[37], E. Kasimi[151], C. Kato[62d], J. Katzy[48], S. Kaur[34], K. Kawade[139], K. Kawagoe[88], T. Kawamoto[134], G. Kawamura[55], E.F. Kay[164], F.I. Kaya[157], S. Kazakos[13], V.F. Kazanin[37], Y. Ke[144], J.M. Keaveney[33a], R. Keeler[164], G.V. Kehris[61], J.S. Keller[34], A.S. Kelly[95], D. Kelsey[145], J.J. Kempster[20], K.E. Kennedy[41], P.D. Kennedy[99], O. Kepka[130], B.P. Kerridge[166], S. Kersten[170], B.P. Kerševan[92], S. Keshri[66], L. Keszeghova[28a], S. Ketabchi Haghighat[154], M. Khandoga[126], A. Khanov[120], A.G. Kharlamov[37], T. Kharlamova[37], E.E. Khoda[137], T.J. Khoo[18], G. Khoriauli[165], J. Khubua[148b], Y.A.R. Khwaira[66], M. Kiehn[36], A. Kilgallon[122], D.W. Kim[47a,47b], E. Kim[153], Y.K. Kim[39], N. Kimura[95], A. Kirchhoff[55], D. Kirchmeier[50], C. Kirfel[24], J. Kirk[133], A.E. Kiryunin[109], T. Kishimoto[152], D.P. Kisliuk[154], C. Kitsaki[10], O. Kivernyk[24], M. Klassen[63a], C. Klein[34], L. Klein[165], M.H. Klein[105], M. Klein[91], S.B. Klein[56], U. Klein[91], P. Klimek[36],

A. Klimentov[29], F. Klimpel[109], T. Klingl[24], T. Klioutchnikova[36], F.F. Klitzner[108], P. Kluit[113], S. Kluth[109], E. Kneringer[78], T.M. Knight[154], A. Knue[54], D. Kobayashi[88], R. Kobayashi[86], M. Kocian[142], P. Kodyš[132], D.M. Koeck[145], P.T. Koenig[24], T. Koffas[34], M. Kolb[134], I. Koletsou[4], T. Komarek[121], K. Köneke[54], A.X.Y. Kong[1], T. Kono[117], N. Konstantinidis[95], B. Konya[97], R. Kopeliansky[67], S. Koperny[84a], K. Korcyl[85], K. Kordas[151], G. Koren[150], A. Korn[95], S. Korn[55], I. Korolkov[13], N. Korotkova[37], B. Kortman[113], O. Kortner[109], S. Kortner[109], W.H. Kostecka[114], V.V. Kostyukhin[140], A. Kotsokechagia[134], A. Kotwal[51], A. Koulouris[36], A. Kourkoumeli-Charalampidi[72a,72b], C. Kourkoumelis[9], E. Kourlitis[6], O. Kovanda[145], R. Kowalewski[164], W. Kozanecki[134], A.S. Kozhin[37], V.A. Kramarenko[37], G. Kramberger[92], P. Kramer[99], M.W. Krasny[126], A. Krasznahorkay[36], J.A. Kremer[99], T. Kresse[50], J. Kretzschmar[91], K. Kreul[18], P. Krieger[154], F. Krieter[108], S. Krishnamurthy[102], A. Krishnan[63b], M. Krivos[132], K. Krizka[17a], K. Kroeninger[49], H. Kroha[109], J. Kroll[130], J. Kroll[127], K.S. Krowpman[106], U. Kruchonak[38], H. Krüger[24], N. Krumnack[80], M.C. Kruse[51], J.A. Krzysiak[85], O. Kuchinskaia[37], S. Kuday[3a], D. Kuechler[48], J.T. Kuechler[48], S. Kuehn[36], T. Kuhl[48], V. Kukhtin[38], Y. Kulchitsky[37,a], S. Kuleshov[136d,136b], M. Kumar[33g], N. Kumari[101], A. Kupco[130], T. Kupfer[49], A. Kupich[37], O. Kuprash[54], H. Kurashige[83], L.L. Kurchaninov[155a], Y.A. Kurochkin[37], A. Kurova[37], M. Kuze[153], A.K. Kvam[102], J. Kvita[121], T. Kwan[103], K.W. Kwok[64a], N.G. Kyriacou[105], L.A.O. Laatu[101], C. Lacasta[162], F. Lacava[74a,74b], H. Lacker[18], D. Lacour[126], N.N. Lad[95], E. Ladygin[38], B. Laforge[126], T. Lagouri[136e], S. Lai[55], I.K. Lakomiec[84a], N. Lalloue[60], J.E. Lambert[119], S. Lammers[67], W. Lampl[7], C. Lampoudis[151], A.N. Lancaster[114], E. Lançon[29], U. Landgraf[54], M.P.J. Landon[93], V.S. Lang[54], R.J. Langenberg[102], A.J. Lankford[159], F. Lanni[36], K. Lantzsch[24], A. Lanza[72a], A. Lapertosa[57b,57a], J.F. Laporte[134], T. Lari[70a], F. Lasagni Manghi[23b], M. Lassnig[36], V. Latonova[130], T.S. Lau[64a], A. Laudrain[99], A. Laurier[34], S.D. Lawlor[94], Z. Lawrence[100], M. Lazzaroni[70a,70b], B. Le[100], B. Leban[92], A. Lebedev[80], M. LeBlanc[36], T. LeCompte[6], F. Ledroit-Guillon[60], A.C.A. Lee[95], G.R. Lee[16], L. Lee[61], S.C. Lee[147], S. Lee[47a,47b], T.F. Lee[91], L.L. Leeuw[33c], H.P. Lefebvre[94], M. Lefebvre[164], C. Leggett[17a], K. Lehmann[141], G. Lehmann Miotto[36], M. Leigh[56], W.A. Leight[102], A. Leisos[151,u], M.A.L. Leite[81c], C.E. Leitgeb[48], R. Leitner[132], K.J.C. Leney[44], T. Lenz[24], S. Leone[73a], C. Leonidopoulos[52], A. Leopold[143], C. Leroy[107], R. Les[106], C.G. Lester[32], M. Levchenko[37], J. Levêque[4], D. Levin[105], L.J. Levinson[168], M.P. Lewicki[85], D.J. Lewis[4], A. Li[5], B. Li[14b], B. Li[62b], C. Li[62a], C-Q. Li[62c], H. Li[62a], H. Li[62b], H. Li[14c], H. Li[62b], J. Li[62c], K. Li[137], L. Li[62c], M. Li[14a,14d], Q.Y. Li[62a], S. Li[14a,14d], S. Li[62d,62c,e], T. Li[62b], X. Li[103], Z. Li[62b], Z. Li[125], Z. Li[103], Z. Li[91], Z. Li[14a,14d], Z. Liang[14a], M. Liberatore[48], B. Liberti[75a], K. Lie[64c], J. Lieber Marin[81b], K. Lin[106], R.A. Linck[67], R.E. Lindley[7], J.H. Lindon[2], A. Linss[48], E. Lipeles[127], A. Lipniacka[16], A. Lister[163], J.D. Little[4], B. Liu[14a], B.X. Liu[141], D. Liu[62d,62c], J.B. Liu[62a], J.K.K. Liu[32], K. Liu[62d,62c], M. Liu[62a], M.Y. Liu[62a], P. Liu[14a], Q. Liu[62d,137,62c], X. Liu[62a], Y. Liu[48], Y. Liu[14c,14d], Y.L. Liu[105], Y.W. Liu[62a], M. Livan[72a,72b], J. Llorente Merino[141], S.L. Lloyd[93], E.M. Lobodzinska[48], P. Loch[7], S. Loffredo[75a,75b], T. Lohse[18], K. Lohwasser[138], M. Lokajicek[130,*], J.D. Long[161],

JHEP07(2023)118

I. Longarini[74a,74b], L. Longo[69a,69b], R. Longo[161], I. Lopez Paz[36], A. Lopez Solis[48], J. Lorenz[108], N. Lorenzo Martinez[4], A.M. Lory[108], A. Lösle[54], X. Lou[47a,47b], X. Lou[14a,14d], A. Lounis[66], J. Love[6], P.A. Love[90], J.J. Lozano Bahilo[162], G. Lu[14a,14d], M. Lu[79], S. Lu[127], Y.J. Lu[65], H.J. Lubatti[137], C. Luci[74a,74b], F.L. Lucio Alves[14c], A. Lucotte[60], F. Luehring[67], I. Luise[144], O. Lukianchuk[66], O. Lundberg[143], B. Lund-Jensen[143], N.A. Luongo[122], M.S. Lutz[150], D. Lynn[29], H. Lyons[91], R. Lysak[130], E. Lytken[97], F. Lyu[14a], V. Lyubushkin[38], T. Lyubushkina[38], H. Ma[29], L.L. Ma[62b], Y. Ma[95], D.M. Mac Donell[164], G. Maccarrone[53], J.C. MacDonald[138], R. Madar[40], W.F. Mader[50], J. Maeda[83], T. Maeno[29], M. Maerker[50], V. Magerl[54], H. Maguire[138], D.J. Mahon[41], C. Maidantchik[81b], A. Maio[129a,129b,129d], K. Maj[84a], O. Majersky[28a], S. Majewski[122], N. Makovec[66], V. Maksimovic[15], B. Malaescu[126], Pa. Malecki[85], V.P. Maleev[37], F. Malek[60], D. Malito[43b,43a], U. Mallik[79], C. Malone[32], S. Maltezos[10], S. Malyukov[38], J. Mamuzic[13], G. Mancini[53], G. Manco[72a,72b], J.P. Mandalia[93], I. Mandić[92], L. Manhaes de Andrade Filho[81a], I.M. Maniatis[151], M. Manisha[134], J. Manjarres Ramos[50], D.C. Mankad[168], A. Mann[108], B. Mansoulie[134], S. Manzoni[36], A. Marantis[151,u], G. Marchiori[5], M. Marcisovsky[130], L. Marcoccia[75a,75b], C. Marcon[70a,70b], M. Marinescu[20], M. Marjanovic[119], E.J. Marshall[90], Z. Marshall[17a], S. Marti-Garcia[162], T.A. Martin[166], V.J. Martin[52], B. Martin dit Latour[16], L. Martinelli[74a,74b], M. Martinez[13,v], P. Martinez Agullo[162], V.I. Martinez Outschoorn[102], P. Martinez Suarez[13], S. Martin-Haugh[133], V.S. Martoiu[27b], A.C. Martyniuk[95], A. Marzin[36], S.R. Maschek[109], L. Masetti[99], T. Mashimo[152], J. Masik[100], A.L. Maslennikov[37], L. Massa[23b], P. Massarotti[71a,71b], P. Mastrandrea[73a,73b], A. Mastroberardino[43b,43a], T. Masubuchi[152], T. Mathisen[160], N. Matsuzawa[152], J. Maurer[27b], B. Maček[92], D.A. Maximov[37], R. Mazini[147], I. Maznas[151], M. Mazza[106], S.M. Mazza[135], C. Mc Ginn[29,ak], J.P. Mc Gowan[103], S.P. Mc Kee[105], W.P. McCormack[17a], E.F. McDonald[104], A.E. McDougall[113], J.A. Mcfayden[145], G. Mchedlidze[148b], R.P. Mckenzie[33g], T.C. Mclachlan[48], D.J. Mclaughlin[95], K.D. McLean[164], S.J. McMahon[133], P.C. McNamara[104], C.M. Mcpartland[91], R.A. McPherson[164,x], T. Megy[40], S. Mehlhase[108], A. Mehta[91], B. Meirose[45], D. Melini[149], B.R. Mellado Garcia[33g], A.H. Melo[55], F. Meloni[48], E.D. Mendes Gouveia[129a], A.M. Mendes Jacques Da Costa[20], H.Y. Meng[154], L. Meng[90], S. Menke[109], M. Mentink[36], E. Meoni[43b,43a], C. Merlassino[125], L. Merola[71a,71b], C. Meroni[70a], G. Merz[105], O. Meshkov[37], J.K.R. Meshreki[140], J. Metcalfe[6], A.S. Mete[6], C. Meyer[67], J-P. Meyer[134], M. Michetti[18], R.P. Middleton[133], L. Mijović[52], G. Mikenberg[168], M. Mikestikova[130], M. Mikuž[92], H. Mildner[138], A. Milic[36], C.D. Milke[44], D.W. Miller[39], L.S. Miller[34], A. Milov[168], D.A. Milstead[47a,47b], T. Min[14c], A.A. Minaenko[37], I.A. Minashvili[148b], L. Mince[59], A.I. Mincer[116], B. Mindur[84a], M. Mineev[38], Y. Mino[86], L.M. Mir[13], M. Miralles Lopez[162], M. Mironova[125], M.C. Missio[112], T. Mitani[167], A. Mitra[166], V.A. Mitsou[162], O. Miu[154], P.S. Miyagawa[93], Y. Miyazaki[88], A. Mizukami[82], J.U. Mjörnmark[97], T. Mkrtchyan[63a], T. Mlinarevic[95], M. Mlynarikova[36], T. Moa[47a,47b], S. Mobius[55], K. Mochizuki[107], P. Moder[48], P. Mogg[108], A.F. Mohammed[14a,14d], S. Mohapatra[41], G. Mokgatitswane[33g], B. Mondal[140], S. Mondal[131], K. Mönig[48], E. Monnier[101], L. Monsonis Romero[162],

J. Montejo Berlingen[36], M. Montella[118], F. Monticelli[89], N. Morange[66], A.L. Moreira De Carvalho[129a], M. Moreno Llácer[162], C. Moreno Martinez[56], P. Morettini[57b], S. Morgenstern[166], M. Morii[61], M. Morinaga[152], A.K. Morley[36], F. Morodei[74a,74b], L. Morvaj[36], P. Moschovakos[36], B. Moser[36], M. Mosidze[148b], T. Moskalets[54], P. Moskvitina[112], J. Moss[31,o], E.J.W. Moyse[102], S. Muanza[101], J. Mueller[128], D. Muenstermann[90], R. Müller[19], G.A. Mullier[97], J.J. Mullin[127], D.P. Mungo[154], J.L. Munoz Martinez[13], D. Munoz Perez[162], F.J. Munoz Sanchez[100], M. Murin[100], W.J. Murray[166,133], A. Murrone[70a,70b], J.M. Muse[119], M. Muškinja[17a], C. Mwewa[29], A.G. Myagkov[37,a], A.J. Myers[8], A.A. Myers[128], G. Myers[67], M. Myska[131], B.P. Nachman[17a], O. Nackenhorst[49], A. Nag[50], K. Nagai[125], K. Nagano[82], J.L. Nagle[29,ak], E. Nagy[101], A.M. Nairz[36], Y. Nakahama[82], K. Nakamura[82], H. Nanjo[123], R. Narayan[44], E.A. Narayanan[111], I. Naryshkin[37], M. Naseri[34], C. Nass[24], G. Navarro[22a], J. Navarro-Gonzalez[162], R. Nayak[150], A. Nayaz[18], P.Y. Nechaeva[37], F. Nechansky[48], L. Nedic[125], T.J. Neep[20], A. Negri[72a,72b], M. Negrini[23b], C. Nellist[112], C. Nelson[103], K. Nelson[105], S. Nemecek[130], M. Nessi[36,h], M.S. Neubauer[161], F. Neuhaus[99], J. Neundorf[48], R. Newhouse[163], P.R. Newman[20], C.W. Ng[128], Y.S. Ng[18], Y.W.Y. Ng[48], B. Ngair[35e], H.D.N. Nguyen[107], R.B. Nickerson[125], R. Nicolaidou[134], J. Nielsen[135], M. Niemeyer[55], N. Nikiforou[36], V. Nikolaenko[37,a], I. Nikolic-Audit[126], K. Nikolopoulos[20], P. Nilsson[29], H.R. Nindhito[56], A. Nisati[74a], N. Nishu[2], R. Nisius[109], J-E. Nitschke[50], E.K. Nkadimeng[33g], S.J. Noacco Rosende[89], T. Nobe[152], D.L. Noel[32], Y. Noguchi[86], T. Nommensen[146], M.A. Nomura[29], M.B. Norfolk[138], R.R.B. Norisam[95], B.J. Norman[34], J. Novak[92], T. Novak[48], O. Novgorodova[50], L. Novotny[131], R. Novotny[111], L. Nozka[121], K. Ntekas[159], N.M.J. Nunes De Moura Junior[81b], E. Nurse[95], F.G. Oakham[34,ah], J. Ocariz[126], A. Ochi[83], I. Ochoa[129a], S. Oerdek[160], A. Ogrodnik[84a], A. Oh[100], C.C. Ohm[143], H. Oide[82], R. Oishi[152], M.L. Ojeda[48], Y. Okazaki[86], M.W. O'Keefe[91], Y. Okumura[152], A. Olariu[27b], L.F. Oleiro Seabra[129a], S.A. Olivares Pino[136e], D. Oliveira Damazio[29], D. Oliveira Goncalves[81a], J.L. Oliver[159], M.J.R. Olsson[159], A. Olszewski[85], J. Olszowska[85,*], Ö.O. Öncel[54], D.C. O'Neil[141], A.P. O'Neill[19], A. Onofre[129a,129e], P.U.E. Onyisi[11], M.J. Oreglia[39], G.E. Orellana[89], D. Orestano[76a,76b], N. Orlando[13], R.S. Orr[154], V. O'Shea[59], R. Ospanov[62a], G. Otero y Garzon[30], H. Otono[88], P.S. Ott[63a], G.J. Ottino[17a], M. Ouchrif[35d], J. Ouellette[29,ak], F. Ould-Saada[124], M. Owen[59], R.E. Owen[133], K.Y. Oyulmaz[21a], V.E. Ozcan[21a], N. Ozturk[8], S. Ozturk[21d], J. Pacalt[121], H.A. Pacey[32], K. Pachal[51], A. Pacheco Pages[13], C. Padilla Aranda[13], G. Padovano[74a,74b], S. Pagan Griso[17a], G. Palacino[67], A. Palazzo[69a,69b], S. Palazzo[52], S. Palestini[36], M. Palka[84b], J. Pan[171], T. Pan[64a], D.K. Panchal[11], C.E. Pandini[113], J.G. Panduro Vazquez[94], H. Pang[14b], P. Pani[48], G. Panizzo[68a,68c], L. Paolozzi[56], C. Papadatos[107], S. Parajuli[44], A. Paramonov[6], C. Paraskevopoulos[10], D. Paredes Hernandez[64b], T.H. Park[154], M.A. Parker[32], F. Parodi[57b,57a], E.W. Parrish[114], V.A. Parrish[52], J.A. Parsons[41], U. Parzefall[54], B. Pascual Dias[107], L. Pascual Dominguez[150], V.R. Pascuzzi[17a], F. Pasquali[113], E. Pasqualucci[74a], S. Passaggio[57b], F. Pastore[94], P. Pasuwan[47a,47b], P. Patel[85], J.R. Pater[100], T. Pauly[36], J. Pearkes[142], M. Pedersen[124], R. Pedro[129a], S.V. Peleganchuk[37], O. Penc[36], E.A. Pender[52], C. Peng[64b], H. Peng[62a], K.E. Penski[108],

JHEP07(2023)118

M. Penzin[37], B.S. Peralva[81d], A.P. Pereira Peixoto[60], L. Pereira Sanchez[47a,47b], D.V. Perepelitsa[29,ak], E. Perez Codina[155a], M. Perganti[10], L. Perini[70a,70b,*], H. Pernegger[36], S. Perrella[36], A. Perrevoort[112], O. Perrin[40], K. Peters[48], R.F.Y. Peters[100], B.A. Petersen[36], T.C. Petersen[42], E. Petit[101], V. Petousis[131], C. Petridou[151], A. Petrukhin[140], M. Pettee[17a], N.E. Pettersson[36], A. Petukhov[37], K. Petukhova[132], A. Peyaud[134], R. Pezoa[136f], L. Pezzotti[36], G. Pezzullo[171], T.M. Pham[169], T. Pham[104], P.W. Phillips[133], M.W. Phipps[161], G. Piacquadio[144], E. Pianori[17a], F. Piazza[70a,70b], R. Piegaia[30], D. Pietreanu[27b], A.D. Pilkington[100], M. Pinamonti[68a,68c], J.L. Pinfold[2], B.C. Pinheiro Pereira[129a], C. Pitman Donaldson[95], D.A. Pizzi[34], L. Pizzimento[75a,75b], A. Pizzini[113], M.-A. Pleier[29], V. Plesanovs[54], V. Pleskot[132], E. Plotnikova[38], G. Poddar[4], R. Poettgen[97], L. Poggioli[126], I. Pogrebnyak[106], D. Pohl[24], I. Pokharel[55], S. Polacek[132], G. Polesello[72a], A. Poley[141,155a], R. Polifka[131], A. Polini[23b], C.S. Pollard[125], Z.B. Pollock[118], V. Polychronakos[29], E. Pompa Pacchi[74a,74b], D. Ponomarenko[37], L. Pontecorvo[36], S. Popa[27a], G.A. Popeneciu[27d], D.M. Portillo Quintero[155a], S. Pospisil[131], P. Postolache[27c], K. Potamianos[125], I.N. Potrap[38], C.J. Potter[32], H. Potti[1], T. Poulsen[48], J. Poveda[162], M.E. Pozo Astigarraga[36], A. Prades Ibanez[162], M.M. Prapa[46], J. Pretel[54], D. Price[100], M. Primavera[69a], M.A. Principe Martin[98], R. Privara[121], M.L. Proffitt[137], N. Proklova[127], K. Prokofiev[64c], G. Proto[75a,75b], S. Protopopescu[29], J. Proudfoot[6], M. Przybycien[84a], J.E. Puddefoot[138], D. Pudzha[37], P. Puzo[66], D. Pyatiizbyantseva[37], J. Qian[105], D. Qichen[100], Y. Qin[100], T. Qiu[93], A. Quadt[55], M. Queitsch-Maitland[100], G. Quetant[56], G. Rabanal Bolanos[61], D. Rafanoharana[54], F. Ragusa[70a,70b], J.L. Rainbolt[39], J.A. Raine[56], S. Rajagopalan[29], E. Ramakoti[37], K. Ran[48,14d], N.P. Rapheeha[33g], V. Raskina[126], D.F. Rassloff[63a], S. Rave[99], B. Ravina[55], I. Ravinovich[168], M. Raymond[36], A.L. Read[124], N.P. Readioff[138], D.M. Rebuzzi[72a,72b], G. Redlinger[29], K. Reeves[45], J.A. Reidelsturz[170], D. Reikher[150], A. Reiss[99], A. Rej[140], C. Rembser[36], A. Renardi[48], M. Renda[27b], M.B. Rendel[109], F. Renner[48], A.G. Rennie[59], S. Resconi[70a], M. Ressegotti[57b,57a], E.D. Resseguie[17a], S. Rettie[36], B. Reynolds[118], E. Reynolds[17a], M. Rezaei Estabragh[170], O.L. Rezanova[37], P. Reznicek[132], E. Ricci[77a,77b], R. Richter[109], S. Richter[47a,47b], E. Richter-Was[84b], M. Ridel[126], P. Rieck[116], P. Riedler[36], M. Rijssenbeek[144], A. Rimoldi[72a,72b], M. Rimoldi[48], L. Rinaldi[23b,23a], T.T. Rinn[29], M.P. Rinnagel[108], G. Ripellino[143], I. Riu[13], P. Rivadeneira[48], J.C. Rivera Vergara[164], F. Rizatdinova[120], E. Rizvi[93], C. Rizzi[56], B.A. Roberts[166], B.R. Roberts[17a], S.H. Robertson[103,x], M. Robin[48], D. Robinson[32], C.M. Robles Gajardo[136f], M. Robles Manzano[99], A. Robson[59], A. Rocchi[75a,75b], C. Roda[73a,73b], S. Rodriguez Bosca[63a], Y. Rodriguez Garcia[22a], A. Rodriguez Rodriguez[54], A.M. Rodríguez Vera[155b], S. Roe[36], J.T. Roemer[159], A.R. Roepe-Gier[119], J. Roggel[170], O. Røhne[124], R.A. Rojas[164], B. Roland[54], C.P.A. Roland[67], J. Roloff[29], A. Romaniouk[37], E. Romano[72a,72b], M. Romano[23b], A.C. Romero Hernandez[161], N. Rompotis[91], L. Roos[126], S. Rosati[74a], B.J. Rosser[39], E. Rossi[4], E. Rossi[71a,71b], L.P. Rossi[57b], L. Rossini[48], R. Rosten[118], M. Rotaru[27b], B. Rottler[54], D. Rousseau[66], D. Rousso[32], G. Rovelli[72a,72b], A. Roy[161], A. Rozanov[101], Y. Rozen[149], X. Ruan[33g], A. Rubio Jimenez[162], A.J. Ruby[91], V.H. Ruelas Rivera[18],

JHEP07(2023)118

T.A. Ruggeri[1], F. Rühr[54], A. Ruiz-Martinez[162], A. Rummler[36], Z. Rurikova[54], N.A. Rusakovich[38], H.L. Russell[164], J.P. Rutherfoord[7], K. Rybacki[90], M. Rybar[132], E.B. Rye[124], A. Ryzhov[37], J.A. Sabater Iglesias[56], P. Sabatini[162], L. Sabetta[74a,74b], H.F-W. Sadrozinski[135], F. Safai Tehrani[74a], B. Safarzadeh Samani[145], M. Safdari[142], S. Saha[103], M. Sahinsoy[109], M. Saimpert[134], M. Saito[152], T. Saito[152], D. Salamani[36], G. Salamanna[76a,76b], A. Salnikov[142], J. Salt[162], A. Salvador Salas[13], D. Salvatore[43b,43a], F. Salvatore[145], A. Salzburger[36], D. Sammel[54], D. Sampsonidis[151], D. Sampsonidou[62d,62c], J. Sánchez[162], A. Sanchez Pineda[4], V. Sanchez Sebastian[162], H. Sandaker[124], C.O. Sander[48], J.A. Sandesara[102], M. Sandhoff[170], C. Sandoval[22b], D.P.C. Sankey[133], A. Sansoni[53], L. Santi[74a,74b], C. Santoni[40], H. Santos[129a,129b], S.N. Santpur[17a], A. Santra[168], K.A. Saoucha[138], J.G. Saraiva[129a,129d], J. Sardain[7], O. Sasaki[82], K. Sato[156], C. Sauer[63b], F. Sauerburger[54], E. Sauvan[4], P. Savard[154,ah], R. Sawada[152], C. Sawyer[133], L. Sawyer[96], I. Sayago Galvan[162], C. Sbarra[23b], A. Sbrizzi[23b,23a], T. Scanlon[95], J. Schaarschmidt[137], P. Schacht[109], D. Schaefer[39], U. Schäfer[99], A.C. Schaffer[66], D. Schaile[108], R.D. Schamberger[144], E. Schanet[108], C. Scharf[18], M.M. Schefer[19], V.A. Schegelsky[37], D. Scheirich[132], F. Schenck[18], M. Schernau[159], C. Scheulen[55], C. Schiavi[57b,57a], Z.M. Schillaci[26], E.J. Schioppa[69a,69b], M. Schioppa[43b,43a], B. Schlag[99], K.E. Schleicher[54], S. Schlenker[36], J. Schmeing[170], M.A. Schmidt[170], K. Schmieden[99], C. Schmitt[99], S. Schmitt[48], L. Schoeffel[134], A. Schoening[63b], P.G. Scholer[54], E. Schopf[125], M. Schott[99], J. Schovancova[36], S. Schramm[56], F. Schroeder[170], H-C. Schultz-Coulon[63a], M. Schumacher[54], B.A. Schumm[135], Ph. Schune[134], A. Schwartzman[142], T.A. Schwarz[105], Ph. Schwemling[134], R. Schwienhorst[106], A. Sciandra[135], G. Sciolla[26], F. Scuri[73a], F. Scutti[104], C.D. Sebastiani[91], K. Sedlaczek[49], P. Seema[18], S.C. Seidel[111], A. Seiden[135], B.D. Seidlitz[41], T. Seiss[39], C. Seitz[48], J.M. Seixas[81b], G. Sekhniaidze[71a], S.J. Sekula[44], L. Selem[4], N. Semprini-Cesari[23b,23a], S. Sen[51], D. Sengupta[56], V. Senthilkumar[162], L. Serin[66], L. Serkin[68a,68b], M. Sessa[76a,76b], H. Severini[119], S. Sevova[142], F. Sforza[57b,57a], A. Sfyrla[56], E. Shabalina[55], R. Shaheen[143], J.D. Shahinian[127], D. Shaked Renous[168], L.Y. Shan[14a], M. Shapiro[17a], A. Sharma[36], A.S. Sharma[163], P. Sharma[79], S. Sharma[48], P.B. Shatalov[37], K. Shaw[145], S.M. Shaw[100], Q. Shen[62c,5], P. Sherwood[95], L. Shi[95], C.O. Shimmin[171], Y. Shimogama[167], J.D. Shinner[94], I.P.J. Shipsey[125], S. Shirabe[60], M. Shiyakova[38], J. Shlomi[168], M.J. Shochet[39], J. Shojaii[104], D.R. Shope[124], S. Shrestha[118,al], E.M. Shrif[33g], M.J. Shroff[164], P. Sicho[130], A.M. Sickles[161], E. Sideras Haddad[33g], A. Sidoti[23b], F. Siegert[50], Dj. Sijacki[15], R. Sikora[84a], F. Sili[89], J.M. Silva[20], M.V. Silva Oliveira[36], S.B. Silverstein[47a], S. Simion[66], R. Simoniello[36], E.L. Simpson[59], N.D. Simpson[97], S. Simsek[21d], S. Sindhu[55], P. Sinervo[154], V. Sinetckii[37], S. Singh[141], S. Singh[154], S. Sinha[48], S. Sinha[33g], M. Sioli[23b,23a], I. Siral[36], S.Yu. Sivoklokov[37,*], J. Sjölin[47a,47b], A. Skaf[55], E. Skorda[97], P. Skubic[119], M. Slawinska[85], V. Smakhtin[168], B.H. Smart[133], J. Smiesko[36], S.Yu. Smirnov[37], Y. Smirnov[37], L.N. Smirnova[37,a], O. Smirnova[97], A.C. Smith[41], E.A. Smith[39], H.A. Smith[125], J.L. Smith[91], R. Smith[142], M. Smizanska[90], K. Smolek[131], A. Smykiewicz[85], A.A. Snesarev[37], H.L. Snoek[113], S. Snyder[29], R. Sobie[164,x], A. Soffer[150], C.A. Solans Sanchez[36], E.Yu. Soldatov[37], U. Soldevila[162],

JHEP07(2023)118

A.A. Solodkov[37], S. Solomon[54], A. Soloshenko[38], K. Solovieva[54], O.V. Solovyanov[37], V. Solovyev[37], P. Sommer[36], A. Sonay[13], W.Y. Song[155b], A. Sopczak[131], A.L. Sopio[95], F. Sopkova[28b], V. Sothilingam[63a], S. Sottocornola[72a,72b], R. Soualah[115b], Z. Soumaimi[35e], D. South[48], S. Spagnolo[69a,69b], M. Spalla[109], F. Spanò[94], D. Sperlich[54], G. Spigo[36], M. Spina[145], S. Spinali[90], D.P. Spiteri[59], M. Spousta[132], E.J. Staats[34], A. Stabile[70a,70b], R. Stamen[63a], M. Stamenkovic[113], A. Stampekis[20], M. Standke[24], E. Stanecka[85], M.V. Stange[50], B. Stanislaus[17a], M.M. Stanitzki[48], M. Stankaityte[125], B. Stapf[48], E.A. Starchenko[37], G.H. Stark[135], J. Stark[101,ab], D.M. Starko[155b], P. Staroba[130], P. Starovoitov[63a], S. Stärz[103], R. Staszewski[85], G. Stavropoulos[46], J. Steentoft[160], P. Steinberg[29], A.L. Steinhebel[122], B. Stelzer[141,155a], H.J. Stelzer[128], O. Stelzer-Chilton[155a], H. Stenzel[58], T.J. Stevenson[145], G.A. Stewart[36], M.C. Stockton[36], G. Stoicea[27b], M. Stolarski[129a], S. Stonjek[109], A. Straessner[50], J. Strandberg[143], S. Strandberg[47a,47b], M. Strauss[119], T. Strebler[101], P. Strizenec[28b], R. Ströhmer[165], D.M. Strom[122], L.R. Strom[48], R. Stroynowski[44], A. Strubig[47a,47b], S.A. Stucci[29], B. Stugu[16], J. Stupak[119], N.A. Styles[48], D. Su[142], S. Su[62a], W. Su[62d,137,62c], X. Su[62a,66], K. Sugizaki[152], V.V. Sulin[37], M.J. Sullivan[91], D.M.S. Sultan[77a,77b], L. Sultanaliyeva[37], S. Sultansoy[3b], T. Sumida[86], S. Sun[105], S. Sun[169], O. Sunneborn Gudnadottir[160], M.R. Sutton[145], M. Svatos[130], M. Swiatlowski[155a], T. Swirski[165], I. Sykora[28a], M. Sykora[132], T. Sykora[132], D. Ta[99], K. Tackmann[48,w], A. Taffard[159], R. Tafirout[155a], J.S. Tafoya Vargas[66], R.H.M. Taibah[126], R. Takashima[87], K. Takeda[83], E.P. Takeva[52], Y. Takubo[82], M. Talby[101], A.A. Talyshev[37], K.C. Tam[64b], N.M. Tamir[150], A. Tanaka[152], J. Tanaka[152], R. Tanaka[66], M. Tanasini[57b,57a], J. Tang[62c], Z. Tao[163], S. Tapia Araya[80], S. Tapprogge[99], A. Tarek Abouelfadl Mohamed[106], S. Tarem[149], K. Tariq[62b], G. Tarna[101,27b], G.F. Tartarelli[70a], P. Tas[132], M. Tasevsky[130], E. Tassi[43b,43a], A.C. Tate[161], G. Tateno[152], Y. Tayalati[35e], G.N. Taylor[104], W. Taylor[155b], H. Teagle[91], A.S. Tee[169], R. Teixeira De Lima[142], P. Teixeira-Dias[94], J.J. Teoh[154], K. Terashi[152], J. Terron[98], S. Terzo[13], M. Testa[53], R.J. Teuscher[154,x], A. Thaler[78], O. Theiner[56], N. Themistokleous[52], T. Theveneaux-Pelzer[18], O. Thielmann[170], D.W. Thomas[94], J.P. Thomas[20], E.A. Thompson[48], P.D. Thompson[20], E. Thomson[127], E.J. Thorpe[93], Y. Tian[55], V. Tikhomirov[37,a], Yu.A. Tikhonov[37], S. Timoshenko[37], E.X.L. Ting[1], P. Tipton[171], S. Tisserant[101], S.H. Tlou[33g], A. Thourji[40], K. Todome[23b,23a], S. Todorova-Nova[132], S. Todt[50], M. Togawa[82], J. Tojo[88], S. Tokár[28a], K. Tokushuku[82], R. Tombs[32], M. Tomoto[82,110], L. Tompkins[142,q], K.W. Topolnicki[84b], P. Tornambe[102], E. Torrence[122], H. Torres[50], E. Torró Pastor[162], M. Toscani[30], C. Tosciri[39], M. Tost[11], D.R. Tovey[138], A. Traeet[16], I.S. Trandafir[27b], T. Trefzger[165], A. Tricoli[29], I.M. Trigger[155a], S. Trincaz-Duvoid[126], D.A. Trischuk[26], B. Trocmé[60], A. Trofymov[66], C. Troncon[70a], L. Truong[33c], M. Trzebinski[85], A. Trzupek[85], F. Tsai[144], M. Tsai[105], A. Tsiamis[151], P.V. Tsiareshka[37], S. Tsigaridas[155a], A. Tsirigotis[151,u], V. Tsiskaridze[144], E.G. Tskhadadze[148a], M. Tsopoulou[151], Y. Tsujikawa[86], I.I. Tsukerman[37], V. Tsulaia[17a], S. Tsuno[82], O. Tsur[149], D. Tsybychev[144], Y. Tu[64b], A. Tudorache[27b], V. Tudorache[27b], A.N. Tuna[36], S. Turchikhin[38], I. Turk Cakir[3a], R. Turra[70a], T. Turtuvshin[38,y], P.M. Tuts[41], S. Tzamarias[151], P. Tzanis[10], E. Tzovara[99], K. Uchida[152], F. Ukegawa[156],

JHEP07(2023)118

P.A. Ulloa Poblete[136c], G. Unal[36], M. Unal[11], A. Undrus[29], G. Unel[159], J. Urban[28b], P. Urquijo[104], G. Usai[8], R. Ushioda[153], M. Usman[107], Z. Uysal[21b], L. Vacavant[101], V. Vacek[131], B. Vachon[103], K.O.H. Vadla[124], T. Vafeiadis[36], A. Vaitkus[95], C. Valderanis[108], E. Valdes Santurio[47a,47b], M. Valente[155a], S. Valentinetti[23b,23a], A. Valero[162], A. Vallier[101,ab], J.A. Valls Ferrer[162], T.R. Van Daalen[137], P. Van Gemmeren[6], M. Van Rijnbach[124,36], S. Van Stroud[95], I. Van Vulpen[113], M. Vanadia[75a,75b], W. Vandelli[36], M. Vandenbroucke[134], E.R. Vandewall[120], D. Vannicola[150], L. Vannoli[57b,57a], R. Vari[74a], E.W. Varnes[7], C. Varni[17a], T. Varol[147], D. Varouchas[66], L. Varriale[162], K.E. Varvell[146], M.E. Vasile[27b], L. Vaslin[40], G.A. Vasquez[164], F. Vazeille[40], T. Vazquez Schroeder[36], J. Veatch[31], V. Vecchio[100], M.J. Veen[102], I. Veliscek[125], L.M. Veloce[154], F. Veloso[129a,129c], S. Veneziano[74a], A. Ventura[69a,69b], A. Verbytskyi[109], M. Verducci[73a,73b], C. Vergis[24], M. Verissimo De Araujo[81b], W. Verkerke[113], J.C. Vermeulen[113], C. Vernieri[142], P.J. Verschuuren[94], M. Vessella[102], M.C. Vetterli[141,ah], A. Vgenopoulos[151], N. Viaux Maira[136f], T. Vickey[138], O.E. Vickey Boeriu[138], G.H.A. Viehhauser[125], L. Vigani[63b], M. Villa[23b,23a], M. Villaplana Perez[162], E.M. Villhauer[52], E. Vilucchi[53], M.G. Vincter[34], G.S. Virdee[20], A. Vishwakarma[52], C. Vittori[23b,23a], I. Vivarelli[145], V. Vladimirov[166], E. Voevodina[109], F. Vogel[108], P. Vokac[131], J. Von Ahnen[48], E. Von Toerne[24], B. Vormwald[36], V. Vorobel[132], K. Vorobev[37], M. Vos[162], J.H. Vossebeld[91], M. Vozak[113], L. Vozdecky[93], N. Vranjes[15], M. Vranjes Milosavljevic[15], M. Vreeswijk[113], R. Vuillermet[36], O. Vujinovic[99], I. Vukotic[39], S. Wada[156], C. Wagner[102], W. Wagner[170], S. Wahdan[170], H. Wahlberg[89], R. Wakasa[156], M. Wakida[110], V.M. Walbrecht[109], J. Walder[133], R. Walker[108], W. Walkowiak[140], A.M. Wang[61], A.Z. Wang[169], C. Wang[62a], C. Wang[62c], H. Wang[17a], J. Wang[64a], R.-J. Wang[99], R. Wang[61], R. Wang[6], S.M. Wang[147], S. Wang[62b], T. Wang[62a], W.T. Wang[79], X. Wang[14c], X. Wang[161], X. Wang[62c], Y. Wang[62d], Y. Wang[14c], Z. Wang[105], Z. Wang[62d,51,62c], Z. Wang[105], A. Warburton[103], R.J. Ward[20], N. Warrack[59], A.T. Watson[20], H. Watson[59], M.F. Watson[20], G. Watts[137], B.M. Waugh[95], A.F. Webb[11], C. Weber[29], H.A. Weber[18], M.S. Weber[19], S.M. Weber[63a], C. Wei[62a], Y. Wei[125], A.R. Weidberg[125], J. Weingarten[49], M. Weirich[99], C. Weiser[54], C.J. Wells[48], T. Wenaus[29], B. Wendland[49], T. Wengler[36], N.S. Wenke[109], N. Wermes[24], M. Wessels[63a], K. Whalen[122], A.M. Wharton[90], A.S. White[61], A. White[8], M.J. White[1], D. Whiteson[159], L. Wickremasinghe[123], W. Wiedenmann[169], C. Wiel[50], M. Wielers[133], N. Wieseotte[99], C. Wiglesworth[42], L.A.M. Wiik-Fuchs[54], D.J. Wilbern[119], H.G. Wilkens[36], D.M. Williams[41], H.H. Williams[127], S. Williams[32], S. Willocq[102], P.J. Windischhofer[125], F. Winklmeier[122], B.T. Winter[54], J.K. Winter[100], M. Wittgen[142], M. Wobisch[96], R. Wölker[125], J. Wollrath[159], M.W. Wolter[85], H. Wolters[129a,129c], V.W.S. Wong[163], A.F. Wongel[48], S.D. Worm[48], B.K. Wosiek[85], K.W. Woźniak[85], K. Wraight[59], J. Wu[14a,14d], M. Wu[64a], M. Wu[112], S.L. Wu[169], X. Wu[56], Y. Wu[62a], Z. Wu[134,62a], J. Wuerzinger[125], T.R. Wyatt[100], B.M. Wynne[52], S. Xella[42], L. Xia[14c], M. Xia[14b], J. Xiang[64c], X. Xiao[105], M. Xie[62a], X. Xie[62a], S. Xin[14a,14d], J. Xiong[17a], I. Xiotidis[145], D. Xu[14a], H. Xu[62a], H. Xu[62a], L. Xu[62a], R. Xu[127], T. Xu[105], W. Xu[105], Y. Xu[14b], Z. Xu[62b], Z. Xu[14a], B. Yabsley[146],

S. Yacoob[33a], N. Yamaguchi[88], Y. Yamaguchi[153], H. Yamauchi[156], T. Yamazaki[17a], Y. Yamazaki[83], J. Yan[62c], S. Yan[125], Z. Yan[25], H.J. Yang[62c,62d], H.T. Yang[62a], S. Yang[62a], T. Yang[64c], X. Yang[62a], X. Yang[14a], Y. Yang[44], Z. Yang[62a,105], W-M. Yao[17a], Y.C. Yap[48], H. Ye[14c], H. Ye[55], J. Ye[44], S. Ye[29], X. Ye[62a], Y. Yeh[95], I. Yeletskikh[38], B.K. Yeo[17a], M.R. Yexley[90], P. Yin[41], K. Yorita[167], S. Younas[27b], C.J.S. Young[54], C. Young[142], M. Yuan[105], R. Yuan[62b,k], L. Yue[95], X. Yue[63a], M. Zaazoua[35e], B. Zabinski[85], E. Zaid[52], T. Zakareishvili[148b], N. Zakharchuk[34], S. Zambito[56], J.A. Zamora Saa[136d,136b], J. Zang[152], D. Zanzi[54], O. Zaplatilek[131], S.V. Zeißner[49], C. Zeitnitz[170], J.C. Zeng[161], D.T. Zenger Jr[26], O. Zenin[37], T. Ženiš[28a], S. Zenz[93], S. Zerradi[35a], D. Zerwas[66], B. Zhang[14c], D.F. Zhang[138], G. Zhang[14b], J. Zhang[62b], J. Zhang[6], K. Zhang[14a,14d], L. Zhang[14c], P. Zhang[14a,14d], R. Zhang[169], S. Zhang[105], T. Zhang[152], X. Zhang[62c], X. Zhang[62b], Y. Zhang[62c,5], Z. Zhang[17a], Z. Zhang[66], H. Zhao[137], P. Zhao[51], T. Zhao[62b], Y. Zhao[135], Z. Zhao[62a], A. Zhemchugov[38], X. Zheng[62a], Z. Zheng[142], D. Zhong[161], B. Zhou[105], C. Zhou[169], H. Zhou[7], N. Zhou[62c], Y. Zhou[7], C.G. Zhu[62b], C. Zhu[14a,14d], H.L. Zhu[62a], H. Zhu[14a], J. Zhu[105], Y. Zhu[62c], Y. Zhu[62a], X. Zhuang[14a], K. Zhukov[37], V. Zhulanov[37], N.I. Zimine[38], J. Zinsser[63b], M. Ziolkowski[140], L. Živković[15], A. Zoccoli[23b,23a], K. Zoch[56], T.G. Zorbas[138], O. Zormpa[46], W. Zou[41], L. Zwalinski[36]

[1] *Department of Physics, University of Adelaide, Adelaide; Australia*
[2] *Department of Physics, University of Alberta, Edmonton AB; Canada*
[3] [(a)] *Department of Physics, Ankara University, Ankara;*[(b)] *Division of Physics, TOBB University of Economics and Technology, Ankara; Türkiye*
[4] *LAPP, Université Savoie Mont Blanc, CNRS/IN2P3, Annecy; France*
[5] *APC, Université Paris Cité, CNRS/IN2P3, Paris; France*
[6] *High Energy Physics Division, Argonne National Laboratory, Argonne IL; United States of America*
[7] *Department of Physics, University of Arizona, Tucson AZ; United States of America*
[8] *Department of Physics, University of Texas at Arlington, Arlington TX; United States of America*
[9] *Physics Department, National and Kapodistrian University of Athens, Athens; Greece*
[10] *Physics Department, National Technical University of Athens, Zografou; Greece*
[11] *Department of Physics, University of Texas at Austin, Austin TX; United States of America*
[12] *Institute of Physics, Azerbaijan Academy of Sciences, Baku; Azerbaijan*
[13] *Institut de Física d'Altes Energies (IFAE), Barcelona Institute of Science and Technology, Barcelona; Spain*
[14] [(a)] *Institute of High Energy Physics, Chinese Academy of Sciences, Beijing;*[(b)] *Physics Department, Tsinghua University, Beijing;*[(c)] *Department of Physics, Nanjing University, Nanjing;*[(d)] *University of Chinese Academy of Science (UCAS), Beijing; China*
[15] *Institute of Physics, University of Belgrade, Belgrade; Serbia*
[16] *Department for Physics and Technology, University of Bergen, Bergen; Norway*
[17] [(a)] *Physics Division, Lawrence Berkeley National Laboratory, Berkeley CA;*[(b)] *University of California, Berkeley CA; United States of America*
[18] *Institut für Physik, Humboldt Universität zu Berlin, Berlin; Germany*
[19] *Albert Einstein Center for Fundamental Physics and Laboratory for High Energy Physics, University of Bern, Bern; Switzerland*
[20] *School of Physics and Astronomy, University of Birmingham, Birmingham; United Kingdom*
[21] [(a)] *Department of Physics, Bogazici University, Istanbul;*[(b)] *Department of Physics Engineering, Gaziantep University, Gaziantep;*[(c)] *Department of Physics, Istanbul University, Istanbul;*[(d)] *Istinye University, Sariyer, Istanbul; Türkiye*

JHEP07(2023)118

22 (a) Facultad de Ciencias y Centro de Investigaciónes, Universidad Antonio Nariño, Bogotá;(b) Departamento de Física, Universidad Nacional de Colombia, Bogotá; Colombia
23 (a) Dipartimento di Fisica e Astronomia A. Righi, Università di Bologna, Bologna;(b) INFN Sezione di Bologna; Italy
24 Physikalisches Institut, Universität Bonn, Bonn; Germany
25 Department of Physics, Boston University, Boston MA; United States of America
26 Department of Physics, Brandeis University, Waltham MA; United States of America
27 (a) Transilvania University of Brasov, Brasov;(b) Horia Hulubei National Institute of Physics and Nuclear Engineering, Bucharest;(c) Department of Physics, Alexandru Ioan Cuza University of Iasi, Iasi;(d) National Institute for Research and Development of Isotopic and Molecular Technologies, Physics Department, Cluj-Napoca;(e) University Politehnica Bucharest, Bucharest;(f) West University in Timisoara, Timisoara;(g) Faculty of Physics, University of Bucharest, Bucharest; Romania
28 (a) Faculty of Mathematics, Physics and Informatics, Comenius University, Bratislava;(b) Department of Subnuclear Physics, Institute of Experimental Physics of the Slovak Academy of Sciences, Kosice; Slovak Republic
29 Physics Department, Brookhaven National Laboratory, Upton NY; United States of America
30 Universidad de Buenos Aires, Facultad de Ciencias Exactas y Naturales, Departamento de Física, y CONICET, Instituto de Física de Buenos Aires (IFIBA), Buenos Aires; Argentina
31 California State University, CA; United States of America
32 Cavendish Laboratory, University of Cambridge, Cambridge; United Kingdom
33 (a) Department of Physics, University of Cape Town, Cape Town;(b) iThemba Labs, Western Cape;(c) Department of Mechanical Engineering Science, University of Johannesburg, Johannesburg;(d) National Institute of Physics, University of the Philippines Diliman (Philippines);(e) University of South Africa, Department of Physics, Pretoria;(f) University of Zululand, KwaDlangezwa;(g) School of Physics, University of the Witwatersrand, Johannesburg; South Africa
34 Department of Physics, Carleton University, Ottawa ON; Canada
35 (a) Faculté des Sciences Ain Chock, Réseau Universitaire de Physique des Hautes Energies — Université Hassan II, Casablanca;(b) Faculté des Sciences, Université Ibn-Tofail, Kénitra;(c) Faculté des Sciences Semlalia, Université Cadi Ayyad, LPHEA-Marrakech;(d) LPMR, Faculté des Sciences, Université Mohamed Premier, Oujda;(e) Faculté des sciences, Université Mohammed V, Rabat;(f) Institute of Applied Physics, Mohammed VI Polytechnic University, Ben Guerir; Morocco
36 CERN, Geneva; Switzerland
37 Affiliated with an institute covered by a cooperation agreement with CERN
38 Affiliated with an international laboratory covered by a cooperation agreement with CERN
39 Enrico Fermi Institute, University of Chicago, Chicago IL; United States of America
40 LPC, Université Clermont Auvergne, CNRS/IN2P3, Clermont-Ferrand; France
41 Nevis Laboratory, Columbia University, Irvington NY; United States of America
42 Niels Bohr Institute, University of Copenhagen, Copenhagen; Denmark
43 (a) Dipartimento di Fisica, Università della Calabria, Rende;(b) INFN Gruppo Collegato di Cosenza, Laboratori Nazionali di Frascati; Italy
44 Physics Department, Southern Methodist University, Dallas TX; United States of America
45 Physics Department, University of Texas at Dallas, Richardson TX; United States of America
46 National Centre for Scientific Research “Demokritos”, Agia Paraskevi; Greece
47 (a) Department of Physics, Stockholm University;(b) Oskar Klein Centre, Stockholm; Sweden
48 Deutsches Elektronen-Synchrotron DESY, Hamburg and Zeuthen; Germany
49 Fakultät Physik, Technische Universität Dortmund, Dortmund; Germany
50 Institut für Kern- und Teilchenphysik, Technische Universität Dresden, Dresden; Germany
51 Department of Physics, Duke University, Durham NC; United States of America
52 SUPA — School of Physics and Astronomy, University of Edinburgh, Edinburgh; United Kingdom
53 INFN e Laboratori Nazionali di Frascati, Frascati; Italy
54 Physikalisches Institut, Albert-Ludwigs-Universität Freiburg, Freiburg; Germany
55 II. Physikalisches Institut, Georg-August-Universität Göttingen, Göttingen; Germany

[56] Département de Physique Nucléaire et Corpusculaire, Université de Genève, Genève; Switzerland
[57] [(a)] Dipartimento di Fisica, Università di Genova, Genova;[(b)] INFN Sezione di Genova; Italy
[58] II. Physikalisches Institut, Justus-Liebig-Universität Giessen, Giessen; Germany
[59] SUPA — School of Physics and Astronomy, University of Glasgow, Glasgow; United Kingdom
[60] LPSC, Université Grenoble Alpes, CNRS/IN2P3, Grenoble INP, Grenoble; France
[61] Laboratory for Particle Physics and Cosmology, Harvard University, Cambridge MA; United States of America
[62] [(a)] Department of Modern Physics and State Key Laboratory of Particle Detection and Electronics, University of Science and Technology of China, Hefei;[(b)] Institute of Frontier and Interdisciplinary Science and Key Laboratory of Particle Physics and Particle Irradiation (MOE), Shandong University, Qingdao;[(c)] School of Physics and Astronomy, Shanghai Jiao Tong University, Key Laboratory for Particle Astrophysics and Cosmology (MOE), SKLPPC, Shanghai;[(d)] Tsung-Dao Lee Institute, Shanghai; China
[63] [(a)] Kirchhoff-Institut für Physik, Ruprecht-Karls-Universität Heidelberg, Heidelberg;[(b)] Physikalisches Institut, Ruprecht-Karls-Universität Heidelberg, Heidelberg; Germany
[64] [(a)] Department of Physics, Chinese University of Hong Kong, Shatin, N.T., Hong Kong;[(b)] Department of Physics, University of Hong Kong, Hong Kong;[(c)] Department of Physics and Institute for Advanced Study, Hong Kong University of Science and Technology, Clear Water Bay, Kowloon, Hong Kong; China
[65] Department of Physics, National Tsing Hua University, Hsinchu; Taiwan
[66] IJCLab, Université Paris-Saclay, CNRS/IN2P3, 91405, Orsay; France
[67] Department of Physics, Indiana University, Bloomington IN; United States of America
[68] [(a)] INFN Gruppo Collegato di Udine, Sezione di Trieste, Udine;[(b)] ICTP, Trieste;[(c)] Dipartimento Politecnico di Ingegneria e Architettura, Università di Udine, Udine; Italy
[69] [(a)] INFN Sezione di Lecce;[(b)] Dipartimento di Matematica e Fisica, Università del Salento, Lecce; Italy
[70] [(a)] INFN Sezione di Milano;[(b)] Dipartimento di Fisica, Università di Milano, Milano; Italy
[71] [(a)] INFN Sezione di Napoli;[(b)] Dipartimento di Fisica, Università di Napoli, Napoli; Italy
[72] [(a)] INFN Sezione di Pavia;[(b)] Dipartimento di Fisica, Università di Pavia, Pavia; Italy
[73] [(a)] INFN Sezione di Pisa;[(b)] Dipartimento di Fisica E. Fermi, Università di Pisa, Pisa; Italy
[74] [(a)] INFN Sezione di Roma;[(b)] Dipartimento di Fisica, Sapienza Università di Roma, Roma; Italy
[75] [(a)] INFN Sezione di Roma Tor Vergata;[(b)] Dipartimento di Fisica, Università di Roma Tor Vergata, Roma; Italy
[76] [(a)] INFN Sezione di Roma Tre;[(b)] Dipartimento di Matematica e Fisica, Università Roma Tre, Roma; Italy
[77] [(a)] INFN-TIFPA;[(b)] Università degli Studi di Trento, Trento; Italy
[78] Universität Innsbruck, Department of Astro and Particle Physics, Innsbruck; Austria
[79] University of Iowa, Iowa City IA; United States of America
[80] Department of Physics and Astronomy, Iowa State University, Ames IA; United States of America
[81] [(a)] Departamento de Engenharia Elétrica, Universidade Federal de Juiz de Fora (UFJF), Juiz de Fora;[(b)] Universidade Federal do Rio De Janeiro COPPE/EE/IF, Rio de Janeiro;[(c)] Instituto de Física, Universidade de São Paulo, São Paulo;[(d)] Rio de Janeiro State University, Rio de Janeiro; Brazil
[82] KEK, High Energy Accelerator Research Organization, Tsukuba; Japan
[83] Graduate School of Science, Kobe University, Kobe; Japan
[84] [(a)] AGH University of Science and Technology, Faculty of Physics and Applied Computer Science, Krakow;[(b)] Marian Smoluchowski Institute of Physics, Jagiellonian University, Krakow; Poland
[85] Institute of Nuclear Physics Polish Academy of Sciences, Krakow; Poland
[86] Faculty of Science, Kyoto University, Kyoto; Japan
[87] Kyoto University of Education, Kyoto; Japan
[88] Research Center for Advanced Particle Physics and Department of Physics, Kyushu University, Fukuoka; Japan
[89] Instituto de Física La Plata, Universidad Nacional de La Plata and CONICET, La Plata; Argentina
[90] Physics Department, Lancaster University, Lancaster; United Kingdom
[91] Oliver Lodge Laboratory, University of Liverpool, Liverpool; United Kingdom

[92] *Department of Experimental Particle Physics, Jožef Stefan Institute and Department of Physics, University of Ljubljana, Ljubljana; Slovenia*
[93] *School of Physics and Astronomy, Queen Mary University of London, London; United Kingdom*
[94] *Department of Physics, Royal Holloway University of London, Egham; United Kingdom*
[95] *Department of Physics and Astronomy, University College London, London; United Kingdom*
[96] *Louisiana Tech University, Ruston LA; United States of America*
[97] *Fysiska institutionen, Lunds universitet, Lund; Sweden*
[98] *Departamento de Física Teorica C-15 and CIAFF, Universidad Autónoma de Madrid, Madrid; Spain*
[99] *Institut für Physik, Universität Mainz, Mainz; Germany*
[100] *School of Physics and Astronomy, University of Manchester, Manchester; United Kingdom*
[101] *CPPM, Aix-Marseille Université, CNRS/IN2P3, Marseille; France*
[102] *Department of Physics, University of Massachusetts, Amherst MA; United States of America*
[103] *Department of Physics, McGill University, Montreal QC; Canada*
[104] *School of Physics, University of Melbourne, Victoria; Australia*
[105] *Department of Physics, University of Michigan, Ann Arbor MI; United States of America*
[106] *Department of Physics and Astronomy, Michigan State University, East Lansing MI; United States of America*
[107] *Group of Particle Physics, University of Montreal, Montreal QC; Canada*
[108] *Fakultät für Physik, Ludwig-Maximilians-Universität München, München; Germany*
[109] *Max-Planck-Institut für Physik (Werner-Heisenberg-Institut), München; Germany*
[110] *Graduate School of Science and Kobayashi-Maskawa Institute, Nagoya University, Nagoya; Japan*
[111] *Department of Physics and Astronomy, University of New Mexico, Albuquerque NM; United States of America*
[112] *Institute for Mathematics, Astrophysics and Particle Physics, Radboud University/Nikhef, Nijmegen; Netherlands*
[113] *Nikhef National Institute for Subatomic Physics and University of Amsterdam, Amsterdam; Netherlands*
[114] *Department of Physics, Northern Illinois University, DeKalb IL; United States of America*
[115] [(a)] *New York University Abu Dhabi, Abu Dhabi;*[(b)] *University of Sharjah, Sharjah; United Arab Emirates*
[116] *Department of Physics, New York University, New York NY; United States of America*
[117] *Ochanomizu University, Otsuka, Bunkyo-ku, Tokyo; Japan*
[118] *Ohio State University, Columbus OH; United States of America*
[119] *Homer L. Dodge Department of Physics and Astronomy, University of Oklahoma, Norman OK; United States of America*
[120] *Department of Physics, Oklahoma State University, Stillwater OK; United States of America*
[121] *Palacký University, Joint Laboratory of Optics, Olomouc; Czech Republic*
[122] *Institute for Fundamental Science, University of Oregon, Eugene, OR; United States of America*
[123] *Graduate School of Science, Osaka University, Osaka; Japan*
[124] *Department of Physics, University of Oslo, Oslo; Norway*
[125] *Department of Physics, Oxford University, Oxford; United Kingdom*
[126] *LPNHE, Sorbonne Université, Université Paris Cité, CNRS/IN2P3, Paris; France*
[127] *Department of Physics, University of Pennsylvania, Philadelphia PA; United States of America*
[128] *Department of Physics and Astronomy, University of Pittsburgh, Pittsburgh PA; United States of America*
[129] [(a)] *Laboratório de Instrumentação e Física Experimental de Partículas — LIP, Lisboa;*[(b)] *Departamento de Física, Faculdade de Ciências, Universidade de Lisboa, Lisboa;*[(c)] *Departamento de Física, Universidade de Coimbra, Coimbra;*[(d)] *Centro de Física Nuclear da Universidade de Lisboa, Lisboa;*[(e)] *Departamento de Física, Universidade do Minho, Braga;*[(f)] *Departamento de Física Teórica y del Cosmos, Universidad de Granada, Granada (Spain);*[(g)] *Departamento de Física, Instituto Superior Técnico, Universidade de Lisboa, Lisboa; Portugal*
[130] *Institute of Physics of the Czech Academy of Sciences, Prague; Czech Republic*
[131] *Czech Technical University in Prague, Prague; Czech Republic*
[132] *Charles University, Faculty of Mathematics and Physics, Prague; Czech Republic*

JHEP07(2023)118

[133] Particle Physics Department, Rutherford Appleton Laboratory, Didcot; United Kingdom
[134] IRFU, CEA, Université Paris-Saclay, Gif-sur-Yvette; France
[135] Santa Cruz Institute for Particle Physics, University of California Santa Cruz, Santa Cruz CA; United States of America
[136] [(a)] Departamento de Física, Pontificia Universidad Católica de Chile, Santiago;[(b)] Millennium Institute for Subatomic physics at high energy frontier (SAPHIR), Santiago;[(c)] Instituto de Investigación Multidisciplinario en Ciencia y Tecnología, y Departamento de Física, Universidad de La Serena;[(d)] Universidad Andres Bello, Department of Physics, Santiago;[(e)] Instituto de Alta Investigación, Universidad de Tarapacá, Arica;[(f)] Departamento de Física, Universidad Técnica Federico Santa María, Valparaíso; Chile
[137] Department of Physics, University of Washington, Seattle WA; United States of America
[138] Department of Physics and Astronomy, University of Sheffield, Sheffield; United Kingdom
[139] Department of Physics, Shinshu University, Nagano; Japan
[140] Department Physik, Universität Siegen, Siegen; Germany
[141] Department of Physics, Simon Fraser University, Burnaby BC; Canada
[142] SLAC National Accelerator Laboratory, Stanford CA; United States of America
[143] Department of Physics, Royal Institute of Technology, Stockholm; Sweden
[144] Departments of Physics and Astronomy, Stony Brook University, Stony Brook NY; United States of America
[145] Department of Physics and Astronomy, University of Sussex, Brighton; United Kingdom
[146] School of Physics, University of Sydney, Sydney; Australia
[147] Institute of Physics, Academia Sinica, Taipei; Taiwan
[148] [(a)] E. Andronikashvili Institute of Physics, Iv. Javakhishvili Tbilisi State University, Tbilisi;[(b)] High Energy Physics Institute, Tbilisi State University, Tbilisi;[(c)] University of Georgia, Tbilisi; Georgia
[149] Department of Physics, Technion, Israel Institute of Technology, Haifa; Israel
[150] Raymond and Beverly Sackler School of Physics and Astronomy, Tel Aviv University, Tel Aviv; Israel
[151] Department of Physics, Aristotle University of Thessaloniki, Thessaloniki; Greece
[152] International Center for Elementary Particle Physics and Department of Physics, University of Tokyo, Tokyo; Japan
[153] Department of Physics, Tokyo Institute of Technology, Tokyo; Japan
[154] Department of Physics, University of Toronto, Toronto ON; Canada
[155] [(a)] TRIUMF, Vancouver BC;[(b)] Department of Physics and Astronomy, York University, Toronto ON; Canada
[156] Division of Physics and Tomonaga Center for the History of the Universe, Faculty of Pure and Applied Sciences, University of Tsukuba, Tsukuba; Japan
[157] Department of Physics and Astronomy, Tufts University, Medford MA; United States of America
[158] United Arab Emirates University, Al Ain; United Arab Emirates
[159] Department of Physics and Astronomy, University of California Irvine, Irvine CA; United States of America
[160] Department of Physics and Astronomy, University of Uppsala, Uppsala; Sweden
[161] Department of Physics, University of Illinois, Urbana IL; United States of America
[162] Instituto de Física Corpuscular (IFIC), Centro Mixto Universidad de Valencia — CSIC, Valencia; Spain
[163] Department of Physics, University of British Columbia, Vancouver BC; Canada
[164] Department of Physics and Astronomy, University of Victoria, Victoria BC; Canada
[165] Fakultät für Physik und Astronomie, Julius-Maximilians-Universität Würzburg, Würzburg; Germany
[166] Department of Physics, University of Warwick, Coventry; United Kingdom
[167] Waseda University, Tokyo; Japan
[168] Department of Particle Physics and Astrophysics, Weizmann Institute of Science, Rehovot; Israel
[169] Department of Physics, University of Wisconsin, Madison WI; United States of America
[170] Fakultät für Mathematik und Naturwissenschaften, Fachgruppe Physik, Bergische Universität Wuppertal, Wuppertal; Germany
[171] Department of Physics, Yale University, New Haven CT; United States of America

[a] *Also Affiliated with an institute covered by a cooperation agreement with CERN*
[b] *Also at An-Najah National University, Nablus; Palestine*
[c] *Also at Borough of Manhattan Community College, City University of New York, New York NY; United States of America*
[d] *Also at Bruno Kessler Foundation, Trento; Italy*
[e] *Also at Center for High Energy Physics, Peking University; China*
[f] *Also at Centro Studi e Ricerche Enrico Fermi; Italy*
[g] *Also at CERN, Geneva; Switzerland*
[h] *Also at Département de Physique Nucléaire et Corpusculaire, Université de Genève, Genève; Switzerland*
[i] *Also at Departament de Fisica de la Universitat Autonoma de Barcelona, Barcelona; Spain*
[j] *Also at Department of Financial and Management Engineering, University of the Aegean, Chios; Greece*
[k] *Also at Department of Physics and Astronomy, Michigan State University, East Lansing MI; United States of America*
[l] *Also at Department of Physics and Astronomy, University of Louisville, Louisville, KY; United States of America*
[m] *Also at Department of Physics, Ben Gurion University of the Negev, Beer Sheva; Israel*
[n] *Also at Department of Physics, California State University, East Bay; United States of America*
[o] *Also at Department of Physics, California State University, Sacramento; United States of America*
[p] *Also at Department of Physics, King's College London, London; United Kingdom*
[q] *Also at Department of Physics, Stanford University, Stanford CA; United States of America*
[r] *Also at Department of Physics, University of Fribourg, Fribourg; Switzerland*
[s] *Also at Department of Physics, University of Thessaly; Greece*
[t] *Also at Department of Physics, Westmont College, Santa Barbara; United States of America*
[u] *Also at Hellenic Open University, Patras; Greece*
[v] *Also at Institucio Catalana de Recerca i Estudis Avancats, ICREA, Barcelona; Spain*
[w] *Also at Institut für Experimentalphysik, Universität Hamburg, Hamburg; Germany*
[x] *Also at Institute of Particle Physics (IPP); Canada*
[y] *Also at Institute of Physics and Technology, Ulaanbaatar; Mongolia*
[z] *Also at Institute of Physics, Azerbaijan Academy of Sciences, Baku; Azerbaijan*
[aa] *Also at Institute of Theoretical Physics, Ilia State University, Tbilisi; Georgia*
[ab] *Also at L2IT, Université de Toulouse, CNRS/IN2P3, UPS, Toulouse; France*
[ac] *Also at Lawrence Livermore National Laboratory, Livermore; United States of America*
[ad] *Also at National Institute of Physics, University of the Philippines Diliman (Philippines); Philippines*
[ae] *Also at RWTH Aachen University, III. Physikalisches Institut A, Aachen; Germany*
[af] *Also at Technical University of Munich, Munich; Germany*
[ag] *Also at The Collaborative Innovation Center of Quantum Matter (CICQM), Beijing; China*
[ah] *Also at TRIUMF, Vancouver BC; Canada*
[ai] *Also at Università di Napoli Parthenope, Napoli; Italy*
[aj] *Also at University of Chinese Academy of Sciences (UCAS), Beijing; China*
[ak] *Also at University of Colorado Boulder, Department of Physics, Colorado; United States of America*
[al] *Also at Washington College, Maryland; United States of America*
[am] *Also at Yeditepe University, Physics Department, Istanbul; Türkiye*
[*] *Deceased*

JHEP07(2023)118